Transportation Research Part F: Psychology and Behaviour 109 (2025) 1313–1333

Contents lists available at ScienceDirect

Transportation Research Part F: Psychology and Behaviour

journal homepage: www.elsevier.com/locate/trf

Ecological data reveal imbalances in human–human collision avoidance due to dyads' social interaction

Adrien Gregorj [a,*], Zeynep Yücel [a,b,c], Francesco Zanlungo [b,d,e], Takayuki Kanda [b,f]

[a] Okayama University, Graduate School of Natural Science and Technology, Division of Industrial Innovation Sciences, 3-1-1 Tsushima-naka, Kita-ku, 700-8530, Okayama, Japan
[b] Advanced Telecommunications Research Institute International, Interaction Science Labs, 2-2-2 Hikaridai, Seika-cho, Soraku-gun, Kyoto, 619-0237, Japan
[c] Ca' Foscari University of Venice, Department of Environmental Sciences, Informatics and Statistics, Scientific Campus, via Torino 155, Mestre, Venice, 30172, Italy
[d] Osaka International Professional University, Department of Informatics, 3-3-1 Umeda, Kita-ku, Osaka, 530-0001, Japan
[e] University of Palermo, Department of Physics and Chemistry Emilio Segrè, Viale delle Scienze, Palermo, 90128, Italy
[f] Kyoto University, Department of Social Informatics, Yoshida-honmachi, Sakyo-ku, Kyoto, 606-8501, Japan

ARTICLE INFO

Dataset link: dyad-single-encounters-article (Original data)

Keywords:
Human–human collision avoidance
Social interactions
Group dynamics
Human navigation
Pedestrian behaviour

ABSTRACT

Humans navigate public spaces safely and smoothly using complex collision avoidance strategies. Traditional models of human–human collision avoidance often draw from physics, relying on repulsive forces, but the effect of social factors on these strategies is not well understood. This study examines frontal encounters between single pedestrians and two-person groups (dyads), investigating the contributions of each party to collision avoidance and the impact of social interaction within the group. Using an ecological dataset of pedestrian trajectories, we measured deviations from a straight path as a proxy for collision avoidance. Our findings reveal a systematic imbalance and significant effects of social interaction on collision avoidance. Single pedestrians tend to prioritise trajectory efficiency in undisturbed situations and are the primary contributors to avoidance during encounters, adjusting their paths according to the dyad's interaction level. For dyads, social interaction correlates with lower efficiency in undisturbed cases and reduced responsiveness during encounters. An analysis of the impact parameter further shows that collision risk influences path deviations: individuals demonstrate larger deviations in response to highly interactive dyads, both in high-risk and less critical encounters. For dyads, the difference in deviation between low and high interaction levels is most pronounced when the single pedestrian is on a near-collision course. These results deepen our understanding of human pedestrian navigation, illustrating dynamical and social implications of group dynamics.

1. Introduction

Human walking motion is studied across various disciplines, each offering a unique perspective, ranging from event safety (von Sivers et al., 2016; Baqui & Löhner, 2019; Ronchi, 2021), and public space design (Francis et al., 2012; Ferrer et al., 2015; Braham

* Corresponding author.
E-mail addresses: adrien.gregorj@s.okayama-u.ac.jp (A. Gregorj), zeynep.yucel@unive.it (Z. Yücel), zanlungo@atr.jp (F. Zanlungo), kanda@i.kyoto-u.ac.jp (T. Kanda).

https://doi.org/10.1016/j.trf.2025.01.039
Received 5 August 2024; Received in revised form 26 January 2025; Accepted 28 January 2025

et al., 2019) to visuo-motor coordination (Patla & Greig, 2006). In this study, we focus on walking as the most fundamental means of transportation (Fruin, 1971) and as an essential activity for independent living. In such settings, people navigate among fellow pedestrians and obstacles, with a focus on safety and fluidity, a concept referred to as human–human collision avoidance. These localised interactions are thought to give rise to self-organization within a local-to-global framework (Rio et al., 2018; Murakami et al., 2021).

To capture the essence of this navigation behaviour, a large variety of computational models have been proposed (Papadimitriou et al., 2009; Löhner, 2010). Early models, inspired by physics, employed repulsive forces to simulate human–human collision avoidance (Helbing & Molnár, 1995). Although these models have been successful in generating coherent patterns at the collective level and have greatly contributed to our understanding of pedestrian motion (Helbing & Molnár, 1995), they often fall short in accurately capturing the realistic attributes of human trajectories (Rio et al., 2018), namely the ones arising from the very fact that humans are social beings, with a theory of mind. For example, it is not unreasonable to assume that pedestrians may adjust their collision avoidance strategies based on social cues from others, an aspect often overlooked in traditional models. More problematically, we believe that there is a shortage of research quantifying the effect of social interaction on pedestrian dynamics in real-world settings.

A typical manifestation of the social nature of humans is group formation. In this study, *groups* refer to 2 or more pedestrians travelling together in the same direction, engaged in a social relationship (McPhail & Wohlstein, 1982; Bugental, 2000). Conversely, pedestrians not part of a group are termed *singles*.[1] We build on the findings of Gregorj et al. (2023, 2024b) that illustrate the effect of social interaction on human–human collision avoidance. Carrying this forward, we investigate the extent of each party's contribution to the collision avoidance and how social interaction affects this contribution by analysing pedestrians' behaviour in their ecological environment. To dissociate the interaction level of groups from their size and hierarchy, we choose to focus on two-person groups, known as *dyads*.[2] We argue that this approach is not oversimplified, as most groups in crowds consist of two people (Schultz et al., 2014) and larger groups often break down into sub-groups of two or three people, making dyads a fundamental building block of crowds (Costa, 2010; Zanlungo & Kanda, 2013). By categorising these dyads according to their level of social interaction (Yücel et al., 2018), we can address the variability in attentional demands and potentially approximate the gradation of mental workload.[3]

2. Literature review

2.1. Community ambulation and cognitive demands

"Community ambulation" refers to the ability to navigate public spaces independently (Bhojwani et al., 2022)[4]. Successful ambulation requires integrating walking with decision-making, processing multimodal sensory information, and adapting to factors such as terrain, traffic density, and attentional demands (Patla & Shumway-Cook, 1999; Cisek & Pastor-Bernier, 2014).

Visual and attentional resources are essential for navigating these environments (Cutting et al., 1995), as they enable pedestrians to anticipate hazards and adapt their movements. However, the principles of anticipatory adaptations in locomotion remain incompletely understood (Gérin-Lajoie et al., 2005). During community ambulation, visual information is processed in real time (Patla & Greig, 2006). This processing is influenced by visual conspicuity (i.e. how easily objects or obstacles stand out in the environment (Itti & Koch, 2000; Gibson, 2014)) and by the specific demands of the task (Torralba et al., 2006). Studies (Patla et al., 2007; Saeedpour-Parizi et al., 2021) have demonstrated that pedestrians rely on visual cues for efficient path planning around static obstacles. This entails utilising visual information to locate the target destination and assess the surrounding path, as well as evaluating the magnitude of the deviation necessary to effectively navigate obstacles, ensuring seamless progression toward their intended destination.

Beyond static obstacles, pedestrians must also be aware of moving targets (i.e. other pedestrians, bicycles, cars, etc.) and anticipate potential collisions, which present greater challenges compared to stationary obstacles due to their momentum and potentially erratic motion (Cinelli & Patla, 2007). Role-dependent strategies in human–human collision avoidance have been shown to vary with factors such as gender, attractiveness, height, and group relationships (Dabbs & Stokes, 1975; van Basten et al., 2009). Conversely, the lack of visual information can increase anxiety during encounters with other pedestrians (Wu & Li, 2022). Additionally, pedestrians navigating around stationary individuals maintain greater distances from males than females, from groups rather than individuals, and from attractive rather than unattractive people (van Basten et al., 2009).

Social interaction in a group typically requires visual resources for tracking the focus of attention (i.e. gaze on partner or a mutual gaze on a target) and eliciting emotions (i.e. facial expression, gestures), etc. Kendon (1990). In addition, the audio channel is essential for understanding speech, detecting changes in pitch, loudness, and intonation of the interlocutor, and managing conversational turns (signaling turn taking, holding, giving or skipping). Given that humans have limited attentional resources and group members may

[1] While each group member can navigate independently, their group affiliation significantly influences their movement. Therefore, we identify and analyse them based on their group dynamics throughout the research.

[2] A dyad specifically refers to a group of exactly two pedestrians. In particular, a pair of pedestrians in a larger group is not considered a dyad in this study.

[3] We would like to clarify that we use the term *interaction* in a specific context, referring exclusively to social interaction characterised by verbal communication, gestures, gaze, physical contact and other forms of engagement within the dyad. Importantly, we distinguish social interaction from the reactive collision avoidance strategies that pedestrians employ during encounters.

[4] A more precise definition provided in Shumway-Cook et al. (2002) specifies that community ambulation entails walking a defined distance (such as 800 m) and navigating stairs without assistance.

already need to devote part of those to the afore-mentioned commitments towards their partners, they are likely to be left with less resources for navigation planning compared to individuals (Zanlungo et al., 2015; Yücel, Zanlungo, et al., 2013; Dam et al., 2023)[5].

2.2. Theory of Mind Model

In addition to the factors discussed, pedestrians' gaze direction is a crucial cue for understanding their intentions and attentional focus (Baron-Cohen et al., 1985). In the context of community ambulation, eye gaze is a key component of social interaction, serving as a communicative tool for signaling intentions and coordinating behaviour (Hessels et al., 2020; Nummenmaa et al., 2009). A study on pedestrian navigation in urban settings by Nummenmaa et al. demonstrated that pedestrians use gaze aversion to signal their intended path, prompting others to steer in the opposite direction to avoid collisions (Nummenmaa et al., 2009).

The Theory of Mind Model suggests that eye gaze plays a crucial role in understanding others' intentions (Baron-Cohen et al., 1985). The absence of gaze alternation can lead to failures in anticipating others' attentional focus and intentions in static scenarios, a phenomenon known as "mind blindness" (Baron-Cohen, 1997). Beyond gaze direction, head orientation indicates focus of attention (Yücel, Salah, et al., 2013) and serves as a cue for path selection, while body orientation suggests a "potential to move" (Zhou et al., 2022). These findings imply that the brain, responsible for orchestrating swift and successful behaviour in such settings, relies not only on spontaneous sensory inputs but also on internal representations of surrounding pedestrians to fulfill this role effectively (Wilson & Golonka, 2013).

2.3. Ecological studies and modelling of pedestrian dynamics

Pedestrian dynamics have been extensively studied through various models (Corbetta & Toschi, 2023) designed to replicate pedestrian behaviour as they navigate toward goals while avoiding both static (i.e. walls, pillars) and dynamic (i.e. other pedestrians) obstacles. Prominent approaches in this field include particle-based simulations (Helbing & Molnár, 1995) and agent-based models (Bonabeau, 2002).

Parameters for these models may be obtained from real-world observations of pedestrians (Zanlungo et al., 2014; Karamouzas et al., 2014), enabling them to more closely mirror actual movement patterns. Recent developments in pedestrian modelling have integrated more complex decision-making processes, inspired by game theory strategies (Bonnemain et al., 2023) or cognitive heuristics (Cristiani et al., 2023; Echeverría-Huarte & Nicolas, 2023).

Data-driven models have gained significant momentum, fueled by the availability of large-scale trajectory datasets captured using increasingly advanced tracking technologies (Bae et al., 2023; Wang et al., 2024). Their rich datasets enable researchers to refine models for better accuracy in capturing real-world pedestrian behaviours, particularly in various scenarios such as navigating along curved paths (van der Vleuten et al., 2024) or avoiding collisions with others (Corbetta et al., 2018).

Human–human collision avoidance remains a central focus in pedestrian dynamics research, often studied in experimental settings involving static obstacles (Jia et al., 2019) or pairwise encounters (Gérin-Lajoie et al., 2005; Huber et al., 2014). These analyses typically involve measuring how much pedestrians deviate from a straight path when navigating around obstacles or others. Works such as Corbetta et al. (2017, 2018) have utilised ecological data, applying methods similar to impact parameter analysis in physics to model pedestrian deviations in both 1-1 and 1-N encounters.

2.4. Present study

Despite extensive research on pedestrian dynamics, several gaps remain unaddressed in the literature. Existing studies have largely focused on individual pedestrian behaviour and basic collision avoidance mechanisms, yet the role of social factors, particularly in group dynamics, has received limited attention. While it is well-established that pedestrians adjust their paths based on static and dynamic obstacles, there is little understanding of how social interactions within groups influence these adjustments. Specifically, there is a lack of research examining how pedestrians perceive and respond to varying levels of social interactions between group members and whether these perceptions influence their own movement strategies.

This study focuses on quantifying the deviations in pedestrian trajectories during encounters as the first step toward modelling how social interactions impact movement strategies. By identifying these deviations, we aim to provide foundational insights that will inform future efforts to model the influence of social dynamics on pedestrian behaviour and collision avoidance.

3. Material and methods

3.1. Dataset

The dataset utilised in this study is the DIAMOR dataset (Kanda & Brščić, 2015), which was previously employed for the purpose of group recognition and pedestrian dynamics modelling (Glas et al., 2014; Yücel et al., 2018). These data were collected in an underground pedestrian street network located in a commercial district of Osaka, Japan. They comprise recordings from two straight

[5] This scenario might also require them to maintain larger personal space to make the trajectory adjustments necessary for collision avoidance (Gérin-Lajoie et al., 2005).

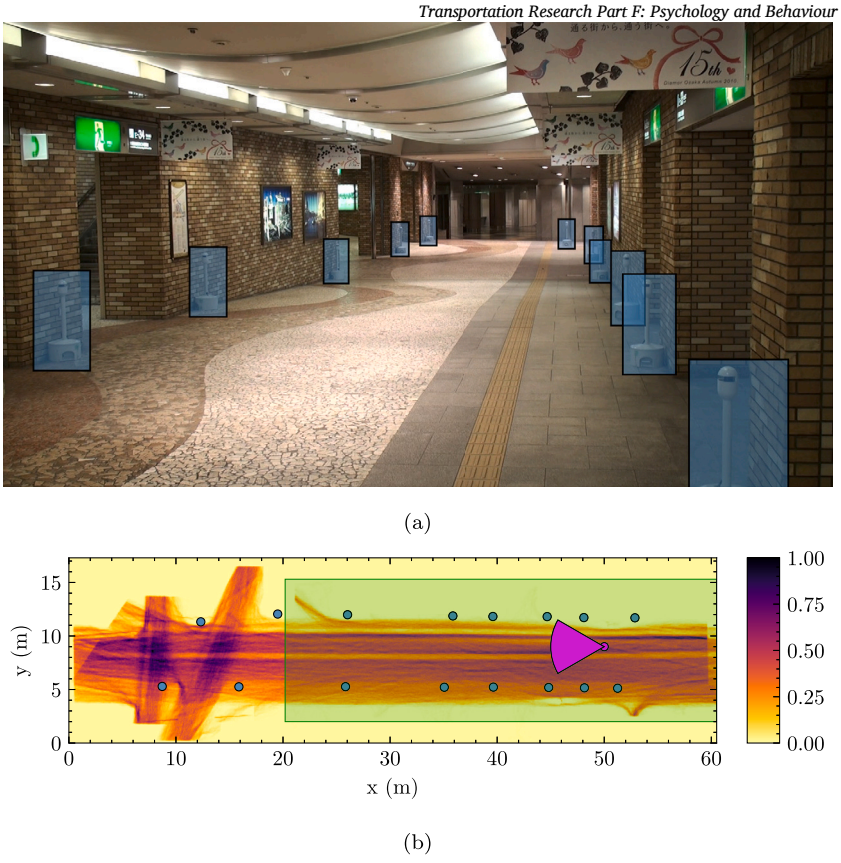

Fig. 1. DIAMOR dataset. (a) Photograph of the underground pedestrian street network where the DIAMOR dataset was recorded. The sensors used for pedestrian tracking are highlighted in blue. (b) Normalised cumulative density map for the DIAMOR dataset. It is obtained by dividing the recording area into a grid of 10 cm × 10 cm cells and counting the number of pedestrians that have been in each cell at any point in time. The counts are then normalised by the maximum count in the grid. Darker areas indicate higher pedestrian density. The green rectangle indicates the portion of the recording area used in this study (a corridor of approximately 40 m), the blue dots represent the sensors used for tracking pedestrians, and the magenta wedge indicates the field of view of the camera used for the video data. (For interpretation of the colours in the figure(s), the reader is referred to the web version of this article.)

corridors within this street network, and our focus centres on one of these. A photograph of the recording area is shown in Fig. 1a. The location, surrounded by several train stations, business centres, and shopping malls, offers diverse pedestrian profiles. The recording area covers roughly 200 m^2 and allows continuous tracking along approximately 50 m and the recording spans eight hours in a weekday.

This dataset is particularly valuable as it captures uninstructed pedestrians in their natural environment, providing insights into naturalistic behaviour. The experiment was reviewed and approved by the ATR ethics board with document number 10-502-1 and was conducted with posters informing passersby about the pedestrian tracking experiment. The data, containing anonymous trajectories derived from range data (Glas et al., 2009), is publicly available (Kanda & Brščić, 2015).

Notably, studies on nonhuman animals have revealed differences in behaviour between constrained tasks and natural settings (Rosenberg et al., 2021; Calhoun et al., 2019; Stringer et al., 2019). Similarly, in human studies, the phenomenon of modifying one's behaviour in response to the awareness of being observed has even been given a name, i.e. the "Hawthorne effect".[6] This effect has been observed in various settings, including when assessing the quality of care provided by trained practitioners (Leonard & Masatu, 2010), or the energy awareness of consumers (Schwartz et al., 2013). In human locomotion, it was shown that observed participants exhibit lower variability in gait parameters (Farhan et al., 2023), and that locomotion parameters (e.g. speed, step length) were impacted by the number of researchers present in the room (Friesen et al., 2020; Farhan et al., 2023). In this respect, the ecological data studied in the upcoming sections minimise experimental or behavioural bias, or subconscious alterations in behaviour, or is at least minimally affected by such factors. Note that with these arguments, we by no means intend to assert that the outcomes derived from traditional, meticulously controlled experimental paradigms are inaccurate or invalid. These approaches, which are proficient at dissecting intricate behaviours into their single components, have significantly contributed to our understanding of the fundamental processes that govern behaviour. Nonetheless, this reductionist approach may constrain the ability to elucidate naturalistic behaviour.

[6] Although it is now largely agreed that such effect was less significant than originally thought in the scenario from which it takes its name (Sedgwick & Greenwood, 2015; McCambridge et al., 2014).

In real-world settings, pristine experiences are more of an exception than the norm and it is essential to study naturalistic behaviour to effectively explain real-world actions (Mobbs et al., 2021).

The data include both depth and video information. The depth information is utilised to derive pedestrian trajectories (Glas et al., 2009), which can be freely downloaded (Kanda & Brščić, 2015). From this tracking process, we obtain the normalised cumulative density map shown in Fig. 1b. The map is obtained by dividing the recording area into a grid of 10 cm × 10 cm cells and counting the number of pedestrians that have been in each cell over time. The counts are then normalised by dividing by the maximum count in the grid, with darker areas indicating higher pedestrian density.

The video data served as the basis for establishing the ground truth regarding dyads and their intensity of interaction. To assess errors arising from coding fatigue and coder bias, each relationship (group membership and interaction intensity) was labelled by two different coders. Initially, coders observed factors such as walking patterns, age, gender, and clothing to determine which pedestrians formed a group (with sizes ranging from two to as many as seven people). In the second stage, coders focused on dyads identified in the first stage to assess interaction intensity. We then used the labels provided by one of the coders as the ground truth. This reduced the amount of data each coder had to view, thus enhancing coding efficiency. Coders were asked to rate the intensity of interaction on a subjective scale from 0 to 3 (0: no interaction, 1: weak interaction, 2: mild interaction, 3: strong interaction). To avoid bias in their assessments, only the resolution (i.e. the number of interaction levels) was predefined (four levels), with no guidelines provided on what constituted weak, mild, or strong interaction intensity. Instead, coders engaged in free-viewing of three hours of dyad video footage to intuitively grasp variations in interaction intensity before starting the actual coding task. A key reason for this approach is that social interactions are inherently fluid and can vary greatly depending on the context, making it difficult to establish strict boundaries for each intensity level. By observing the natural flow of interactions, coders were able to make judgments based on the overall impression, rather than following rigid criteria that might overlook the complexity of social behaviour. The agreement between coders for group relation labelling was evaluated using Cohen's κ coefficient, which showed a high value of $\kappa = 0.96$, indicating strong agreement (Fleiss et al., 2003). For interaction intensity labelling, reliability was assessed using Krippendorff's α coefficient, yielding a value of $\alpha = 0.67$, usually considered sufficiently high (Krippendorff, 2004).

3.2. Data preparation

The raw trajectories in the DIAMOR dataset were sampled at a non-uniform rate, with frequencies ranging from 20 to 50 Hz (Kanda & Brščić, 2015) owing to occlusions or tracking errors. To prevent these inconsistencies from impacting the analysis, we resample the trajectories at a constant rate f_s of 33 Hz using cubic spline interpolation (Knorr et al., 2016).

As mentioned in Section 1, this study focuses on understanding the dynamics of typical single-dyad collision avoidance in public settings. To achieve this, we retain only the trajectories that align with typical walking speeds in public spaces, excluding anomalies. Based on literature on human locomotion (Zanlungo et al., 2014), we consider trajectories with an average velocity falling within the range of $[0.5, 3]$ m/sec as representative of typical urban walking motion while others are associated with different states (such as standing, running, or tracking artifacts).

To address the impact of sensing noise and natural swaying resulting from human gait, we applied filtering to the trajectories. Low-pass filtering is a common method for this (Olivier et al., 2013; Fajen, 2013; Rio et al., 2018), and in this study we opted for a Savitzky–Golay filter (Savitzky & Golay, 1964), which is well-suited for smoothing noisy data. Specifically, we adjusted the polynomial order to 2 and the filter window length to 3 s based on the typical gait cycle duration of 1 to 2 s (Kirtley et al., 1985; Hediyeh et al., 2014).

In this study, we use the notation $\mathbf{p}(t)$ to denote the position of a pedestrian at time t, and $\mathbf{v}(t)$ to denote the velocity of the pedestrian at time t. We will also use the notation $\mathbf{p}_i(t)$ and $\mathbf{v}_i(t)$ to denote the position and velocity of the single i at time t, and $\mathbf{p}_d(t)$ and $\mathbf{v}_d(t)$ to denote the position and velocity of the dyad d at time t.[7]

A *trajectory* T is defined as the sequence of positions $\mathbf{p}(t_k)$ and velocities $\mathbf{v}(t_k)$ of a pedestrian, where t_k is the time at which the positions are recorded, with $k \in [0, N-1]$ and N denoting the number of samples.

The velocity $\mathbf{v}(t_k)$ is derived from the positions using a simple forward Euler difference, i.e.

$$\mathbf{v}(t_k) = \begin{cases} \dfrac{\mathbf{p}(t_{k+1}) - \mathbf{p}(t_k)}{t_{k+1} - t_k} & \text{if } k < N-1 \\ \mathbf{v}(t_{k-1}) & \text{if } k = N-1 \end{cases} \tag{1}$$

$$T = \left[(\mathbf{p}(t_0), \mathbf{v}(t_0)), (\mathbf{p}(t_1), \mathbf{v}(t_1)), \ldots, (\mathbf{p}(t_{N-1}), \mathbf{v}(t_{N-1})) \right]. \tag{2}$$

3.3. Intended direction of motion

Our primary assumption in assessing the trajectory deviation is that pedestrians aim to minimise the distance travelled, selecting the straightest path to reach their destination whenever possible. This assumption, notably introduced by Hoogendoorn and Bovy (2004) and adopted by numerous other studies (Bhojwani et al., 2022; Olivier et al., 2012), posits that at the tactical level, where

[7] When this notation is used, we consider the dyad as a single entity and use the average position and velocity of the dyad members. In other situations, we will consider the dyad members separately to avoid biases from artificial smoothing caused by averaging.

pedestrians make decisions about their desired area and route, they do so by minimising a cost function. This function considers factors such as the distance travelled, trajectory comfort, or anticipated encounters with other pedestrians (Hoogendoorn & Bovy, 2004). In a straight corridor, such as the one examined in our study, a straight line is reasonably the optimal route to cross the corridor (assuming that the pedestrian does not intend to exit the corridor through a side passage). If the corridor is sufficiently wide, the optimal path may still be straight, but not perfectly aligned with the corridor axis, as pedestrians may cross it diagonally.

To compute the straight line trajectory, we first need to identify the *intended direction of motion* of the pedestrian. We define it as the line going through $\mathbf{p}(t_0)$ and guided by $\mathbf{v_0}$ which is the average velocity vector[8] over a 0.5 s window starting at t_0 (the first time point of the trajectory). At a sampling frequency of 33 Hz, this corresponds to $N_e = \lfloor 33 \times 0.5 \rfloor = 16$ samples and

$$\mathbf{v_0} = \frac{1}{N_e} \sum_{k=0}^{N_e-1} \mathbf{v}(t_k). \tag{3}$$

We believe a 0.5 s window size to be appropriate for this analysis. This duration corresponds to the time it takes for a pedestrian to complete a single step, allowing it to effectively capture the overall direction of motion, while being small enough to avoid incorporating the effects of collision avoidance behaviour.

The intended direction of motion L_0 is formally defined as follows:

$$L_0 = \{\mathbf{p}(t_0) + \lambda \mathbf{v_0} \mid \lambda \in \mathbb{R}\}. \tag{4}$$

We argue that this line better represents the intended motion of the pedestrian than one formed by connecting $\mathbf{p}(t_0)$ and $\mathbf{p}(t_{N-1})$, as the latter is influenced by the trajectory deviations that we aim to quantify, particularly if the pedestrian does not return to their original intended path after deviating.

In addition, the *straight line trajectory* T_0 is defined as the trajectory that the pedestrian would follow, should they maintain their intended direction while walking at a constant speed. The points of the straight line trajectory are all on the line L_0 and verify

$$\begin{cases} \tilde{\mathbf{p}}(t_k) = \mathbf{p}(t_0) + \mathbf{v_0} t_k \\ \tilde{\mathbf{v}}(t_k) = \mathbf{v_0} \end{cases} \quad \forall k \in [0, N-1] \tag{5}$$

We emphasise that the straight line trajectory, composed of a sequence of N discrete positions and velocities, differs from the desired direction of motion, which represents a line with an infinite number of points.

3.4. Situations of interest

Drawing from the terminology introduced in Hoogendoorn and Bovy (2004), at the operational level, where pedestrians execute their selected route, they may deviate from the straight line trajectory, possibly influenced by factors such as gait characteristics (Uetake, 1992) and the presence of other pedestrians or obstacles. This study aims to quantify and compare trajectory deviations between singles and dyads, emphasising the impact of social interaction within dyads. We hypothesise that such interactions may influence the mental workload and attentional resources of dyad members, potentially affecting their navigation planning, even though these cognitive factors are not directly measured in this study. We examine two scenarios: (1) undisturbed segments, where singles or dyads move freely without encountering other pedestrians within a reasonably large area, allowing them to move freely without needing to perform avoidance behaviour, and (2) encounters, where a dyad and a single are on a frontal collision or close-to-collision course.

3.4.1. Undisturbed situations

As discussed in Section 3.3, although pedestrians generally aim to minimise the travelled distance by selecting the straightest possible path, it is unrealistic to expect perfectly straight walking even in the absence of other pedestrians. This natural meandering (Uetake, 1992) can be attributed to the natural swaying resulting from human gait and the impact of factors such as the cognitive load (Ho et al., Feb. 28, 2019) and has been modelled using a Langevin-like model (Corbetta et al., 2017).

To establish a baseline of straightness for both individuals and dyads when not forced to avoid collisions, we define undisturbed segments as parts of a trajectory where no other pedestrian is located within 4 m away, consistent with the window size adopted in the computation of trajectory deviation during encounters.

Unlike encounters, which are spatially constrained (typically 3 to 4 m, depending on lateral distance and speed) as defined in Section 3.4.2, undisturbed segments can be arbitrarily long.

To enable comparability between segments from the two scenarios, we must select undisturbed segments with lengths similar to the spatially constrained encounter cases. We extract undisturbed segments of 4 m (Cinelli & Patla, 2008; Karamouzas et al., 2014), ensuring there are no overlaps between them. In addition, the motion direction at the beginning and end of the segment must align with the horizontal axis. This is ensured by verifying that the absolute angles of the velocity vector in 0.5 s windows at the segment's beginning and end, wrapped within the range $[-\pi, \pi]$ are less than $\pi/8$ or greater than $7\pi/8$ in more than 90% of all N_e time steps in these windows. This ensures that the pedestrian is not turning at the beginning or end of the segment.

[8] Since the velocity vectors are computed using a forward Euler difference, the velocity at time t_k points from $\mathbf{p}(t_k)$ to $\mathbf{p}(t_{k+1})$. Therefore, the average velocity vector $\mathbf{v_0}$ points from $\mathbf{p}(t_0)$ to $\mathbf{p}(t_{N_e})$.

Table 1
Trajectory statistics. Breakdown of the number of analysed trajectories. For undisturbed segments, the number of singles and dyad members are shown. Dyads are further broken down according to the intensity of interaction. For encounters, the numbers of situations are shown (each situation involves three trajectories: one for the single and two for the dyad members). The encounters are further broken down according to the intensity of interaction of the dyads. A total of 2768 unique pedestrians were analysed.

Intensity of interaction	Undisturbed		Encounters
	Dyad members	Singles	
0	18	NA	45
1	60		88
2	299		380
3	80		96
All	457	1966	609

According to the above, a single or dyad may have multiple undisturbed segments (in particular if they are observed for a long time and if there are few other pedestrians around). Since these segments might not be independent, given that the pedestrians' behaviour in one segment may be influenced by the behaviour in the previous one, we consider the average deviation across all undisturbed segments of a single or dyad as a unique data point in the analysis. In the "Undisturbed" column Table 1, we list the number of singles and dyads in undisturbed situations. In the "Encounters" column, we provide a breakdown of the number of undisturbed dyads based on the intensity of interaction of the dyad. We note that the number of observations for encounters involving a dyad with an interaction level of 2 is significantly higher than the other levels. This may be partially explained by the "central tendency bias" (Hollingworth, 1910), where coders tend to assign the middle value of the scale more frequently than the extreme values. Nonetheless, we believe that the dataset is sufficiently diverse to draw meaningful conclusions.

3.4.2. Encounters

We define encounters as situations where a dyad d and a single i move toward each other on a collision or close-to-collision course. In these scenarios, it is likely that one or both parties will engage in collision avoidance behaviour to ensure a comfortable passage. Despite the common use of the superposition assumption in many models (such as the social force model (Helbing & Molnár, 1995)), which suggests that the collective effects on a pedestrian from multiple neighbours can be linearly combined (Rio et al., 2018), there is ongoing debate regarding whether neighbourhood is determined by metric or topological distances (e.g. degree of neighbourhood). In this work, we have chosen to use metric distance since the density in our dataset is not high enough to induce collective behaviour (Ballerini et al., 2008). In that respect, we consider only those dyads and singles, who approach each other closely. Specifically, we require that $\exists t \mid d_{di}(t) \leq 4\text{m}$, where d_{di} denotes the instantaneous distance between the dyad and the single.

The choice of a 4 m threshold is grounded in prior research on human–human collision avoidance. Cinelli and Patla found that the "safety zone", or the distance at which individuals begin to avoid a moving object, averages around 3.73 m (Cinelli & Patla, 2008). In addition, Gérin–Lajoie et al. showed that the anticipatory locomotor phase starts with an initial path deviation which occurs approximately 4.5 m from an obstacle (Gérin-Lajoie et al., 2005). It has also been demonstrated that pedestrians focus their gaze most intensely on approaching individuals when they are, on average, approximately 3.97 m away, rarely paying attention to pedestrians at greater distances (Kitazawa & Fujiyama, 2009).

Among the instances where dyads and singles come sufficiently close, we solely consider those engaging in *frontal encounters*, meaning they are moving in opposite directions. There are two main reasons for this selective approach. First, given our focus on human–human collision avoidance within an environment characterised by predominantly bi-directional flow, we argue that encounters involving pedestrians from opposite directions are more pertinent than those moving in the same direction. Second, to understand the implications of social interaction levels (allowing us to speculate on the allocation of attentional demands), we consider only scenarios where the involved parties can visually examine each other (this is crucial for an individual pedestrian to judge group dynamics and assess dyad's interaction level) (Knorr et al., 2016; van Basten et al., 2009). Non-frontal encounters are omitted, since collision avoidance is less prominent for such encounters within low-density bi-directional flow settings, and singles are not likely to react to dyads' characteristics owing to limited observation capabilities.

To address this, we compute the predominant relative motion direction of d and i at the beginning of the encounter by calculating the cosine of the angle between their velocity vectors,

$$c_{di}(t) = \frac{\mathbf{v}_d(t) \cdot \mathbf{v}_i(t)}{||\mathbf{v}_d(t)||||\mathbf{v}_i(t)||}. \tag{6}$$

We classify an encounter as frontal if, during a 0.5 s window starting at t_0, the cosine of the angle between the velocity vectors is smaller than $-\cos(\pi/8)$ for at least 90% of all N_e time steps (indicating an angle range of $[7\pi/8, 9\pi/8]$). This condition is formally expressed as

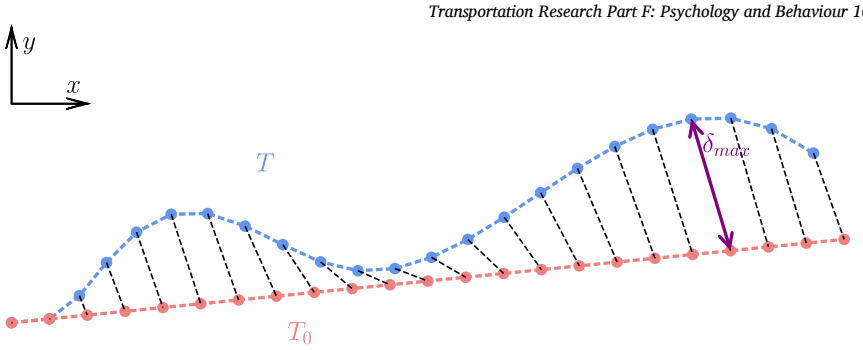

Fig. 2. Lockstep maximum deviation. Illustration of the lockstep maximum deviation, defined as the maximum distance between the simultaneous pairs of points of the observed trajectory T and the straight line trajectory T_0.

$$\frac{1}{N_e}\sum_{k=0}^{N_e-1}\mathbb{1}_{\{c_{di}(t_k)<-\cos(\pi/8)\}} \geq 0.9, \tag{7}$$

where $\mathbb{1}$ is the indicator function that is equal to 1 if the condition inside the brackets is true and 0 otherwise.

To further ensure anticipatory locomotor adjustments during frontal encounters, we calculated extrapolated straight line trajectories (see Eq. (5)) at the initial instant of the encounter and require the closest approach distance on these paths to be less than 2 m. This is because, even when an encounter begins at a distance of 4 m, the dyad and the single might still have sufficient lateral distance to pass each other comfortably, rendering such encounters irrelevant for the scope of this work.

Finally, we ensure that the behaviours of both the dyad and the single are captured even after they have laterally passed each other. This conditioning is motivated by the findings reported by Corbetta et al. (2018), who showed that in very close encounters, lateral distance continues to increase even after avoidance is achieved. To ensure effective clearance between individuals, both the single pedestrian and the dyad must completely move past each other, with sufficiently long trajectories both before and after passing. Specifically, we require them to maintain a distance of at least 3 m apart at the beginning and end of the encounter, indicating an initial approach followed by a subsequent distancing. After applying the conditions described above, the number of encounters subject to an analysis in the upcoming sections, is illustrated in Table 1.

3.5. Measures of deviation

In this section, we define a set of measures for quantifying the deviation of an actual trajectory from an intended straight line trajectory (or, equivalently, its dissimilarity to such a path) along with a discussion on their specifications. For an extensive collection of measures and examples demonstrating how deviation values vary across different types of trajectories, readers can refer to the extended version of this article (Gregorj et al., 2024a).

When computing the deviation of a dyad, we consider the deviation of each member separately. This ensures that the deviation of the dyad is not artificially reduced by averaging the positions of the two members.

3.5.1. Lockstep maximum deviation

In human–human collision avoidance literature, avoidance behaviour is often assessed by measuring deviation from a straight line. In studies with controlled experimental settings, such as frontal encounters in a corridor (Jia et al., 2019; Huber et al., 2014; Daamen et al., 2014), this straight line is considered directly as the axis of the environment and deviation is measured along the orthogonal direction (typically denoted as y-axis). In our case, rather than using the axis of the corridor, we derive an *intended direction of motion* for each single and dyad (see Eqs. (4) and (5)).

The lockstep maximum deviation δ_{max} is defined as the maximum distance between the simultaneous pairs of points of the observed trajectory T and the straight line trajectory T_0. Formally,

$$\delta_{max} = \max_{k\in[0,N-1]} ||\mathbf{p}(t_k) - \tilde{\mathbf{p}}(t_k)||. \tag{8}$$

Notably, this measure is sometimes called the lockstep Euclidean distance in the literature (Tao et al., 2021). In Fig. 2, we show an example for computing the lockstep maximum deviation.

3.5.2. Maximum cumulative turning angle θ_{max}

In addition to the position-based measure δ_{max}, we introduce a measure that quantifies the trajectory deviation of a pedestrian from a straight line trajectory based on the orientation of the velocity vectors, i.e. the direction of motion.

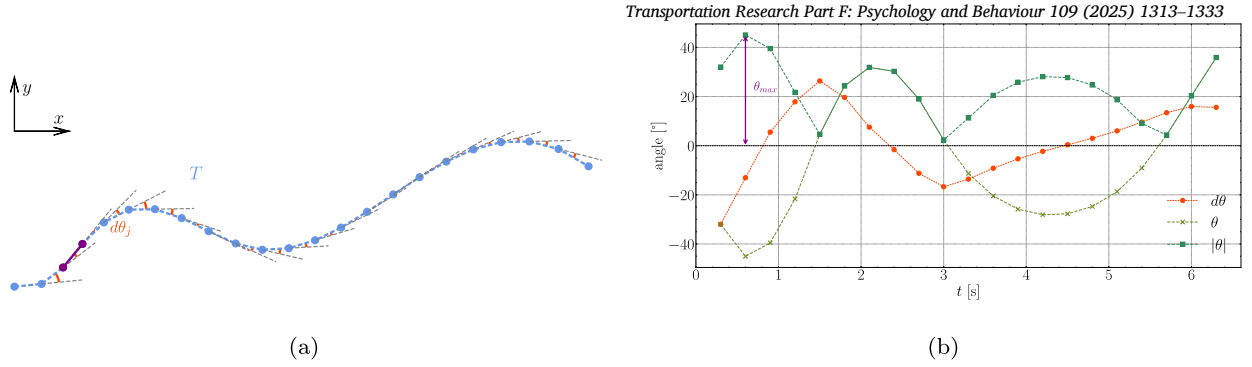

Fig. 3. Maximum cumulative turning angle. (a) Turning angles $d\theta$ are shown in red. The trajectory segment for which the cumulative turning angle is maximum is drawn in purple. (b) Corresponding values of the turning angles $d\theta$, the cumulative turning angles θ, their absolute values $|\theta|$ and the maximum cumulative turning angle θ_{max}.

To deviate from their intended trajectory, pedestrians must naturally turn. We can quantify this deviation by examining the amount of turning performed. The cumulative turning angle until time t_k is defined as the sum of the turning angles between consecutive velocity vectors until time t_k.[9]

Formally, it is defined as

$$\theta_k = \sum_{j=0}^{k-1} d\theta_j, \tag{9}$$

where $d\theta_j$ is the signed angle between the velocity vectors $\mathbf{v}(t_j)$ and $\mathbf{v}(t_{j+1})$, $d\theta_j = \angle(\mathbf{v}(t_j), \mathbf{v}(t_{j+1}))$.

The turning angles are signed, meaning that the cumulative turning angle can be positive or negative, depending on the turning direction (see Fig. 3). We are interested in the maximum cumulative turning angle θ_{max}, which is the maximum of the absolute value of the cumulative turning angles over the trajectory.

$$\theta_{max} = \max_{k\in[0,N-3]} |\theta_k|. \tag{10}$$

In Fig. 3, we illustrate the computation of the maximum cumulative turning angle. The left panel of the figure shows the turning angles $d\theta_j$ and the trajectory segment where the cumulative turning angle is maximum. The right part displays a graph of the turning angles $d\theta_j$, the cumulative turning angles θ_k, $|\theta_k|$, and the maximum cumulative turning angle θ_{max}.

Notably, unlike the lockstep maximum deviation, the maximum cumulative turning angle serves as an early indicator of trajectory deviation. Typically, this maximum is reached earlier in the trajectory than δ_{max}. Specifically, as the pedestrian begins to turn back toward their intended motion direction, the cumulative turning angle starts to decrease.

3.5.3. Turn intensity I

Some studies have proposed measures that combine position and orientation information to quantify a trajectory's deviation. In this section, we present one such measure, namely the turn intensity.

Turn intensity was introduced in Murakami et al. (2021). In the authors' experiment, participants moved and crossed paths along a straight elongated path (x-axis). The authors considered instants at which the motion along the orthogonal axis (y-axis) changes direction, referred to as "turning" instants. A "step" is defined as the motion between two consecutive turning instants, with the "step length" being the y component of a step and the "step angle" the absolute angle deviation from the horizontal axis. Turn intensity is then defined as the product of the step length and the step angle.

In our study, since pedestrians might not be moving along the environment axis (i.e. x axis), we adapt the definitions of turning instants and steps to account for deviation from the intended direction of motion. In particular, we consider the signed angle ψ_k between the initial velocity vector $\mathbf{v_0}$ and the velocity vector $\mathbf{v}(t_k)$ at each time step t_k, $\psi_k = \angle(\mathbf{v_0}, \mathbf{v}(t_k))$. Turning instants t_s are then defined as the moments at which ψ_k changes sign.

We define the s-th step angle ω_s as the absolute value of the angle deviation of a step from the intended motion direction and the step length λ_s as the orthogonal distance between the pedestrian's position at the end of the step and the intended motion direction.

$$\omega_s = \left|\angle(\mathbf{v_0}, (\mathbf{p_{s+1}} - \mathbf{p_s}))\right|, \tag{11}$$

$$\lambda_s = \frac{||(\mathbf{p_{s+1}} - \mathbf{p_s}) \times \mathbf{v_0}||}{||\mathbf{v_0}||}. \tag{12}$$

[9] It is worth noting that this calculation is not the same as simply measuring the angle between $\mathbf{v}(t_0)$ and $\mathbf{v}(t_k)$. In theory, a pedestrian could achieve an angle larger than 2π if they make a full turn. Nonetheless, such situations are unlikely to occur in practice.

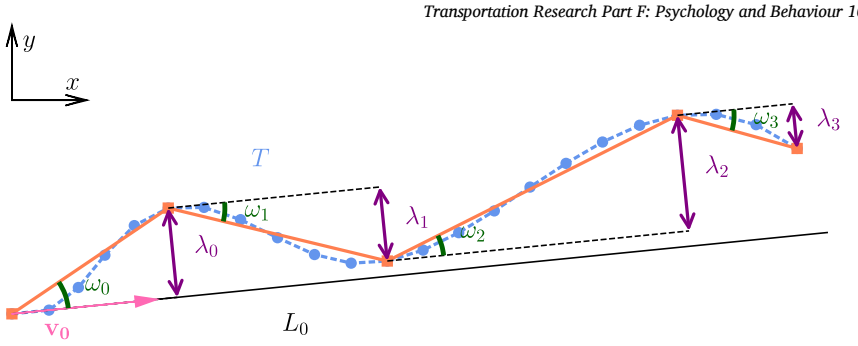

Fig. 4. Turn intensity. Illustration of the variables used in computing the turn intensity I. The steps are shown in orange, the step angles ω are depicted in green, and the step lengths λ are illustrated in purple. (For interpretation of the colours in the figure(s), the reader is referred to the web version of this article.)

The turn intensity is then defined as the average value of the product of the step lengths and step angles,

$$I = \frac{\sum_{s=0}^{N_S-1} \omega_s \lambda_s}{N_S}, \tag{13}$$

where N_S is the number of steps.

In Fig. 4, we illustrate the variables used in computing the turn intensity I.

3.6. Impact parameter

In this section, we briefly introduce the concept of the impact parameter, which has been used in previous analyses of human–human collision avoidance behaviour (Gregorj et al., 2023).

In physics, the impact parameter refers to the distance between the path of an incoming particle and a target particle. Applying this concept to pedestrian trajectories, we treat the deviation of a single from a dyad as a scattering event. To do so, we transform the trajectories of both the dyad d and the single i into a reference frame moving with the dyad. Specifically, at each time instant, the positions of the dyad and the single are translated so that the dyad's centre of mass is positioned at the origin, and their velocities are rotated to align the dyad's movement with the positive x-axis. We denote the position of a single in the reference frame as $\hat{\mathbf{p}}_i$ and its velocity as $\hat{\mathbf{v}}_i$.

In this reference frame, the impact parameter r_b is computed as the distance from the dyad (positioned at the origin) to the line guided by the single's velocity vectors at the beginning of the encounter (as in Section 3.3, we average the velocity vectors over N_e time instants to alleviate the impact of orientation noise). The impact parameter can be considered to indicate how close the single and the dyad would have approached each other without collision avoidance. We illustrate the computation of the impact parameter in Fig. 5.

Let $\hat{\mathbf{v}}_{i_0}$ be the average velocity vector of the single over the first N_e time instants of the encounter,

$$\hat{\mathbf{v}}_{i_0} = \frac{1}{N_e} \sum_{k=0}^{N_e-1} \hat{\mathbf{v}}_i(t_k). \tag{14}$$

We can compute r_b as

$$r_b = \frac{||\hat{\mathbf{v}}_{i_0} \times \hat{\mathbf{p}}_i(t_0)||}{||\hat{\mathbf{v}}_{i_0}||}. \tag{15}$$

As detailed in Gregorj et al. (2023), we scale the impact parameter by the dyad's width (i.e. the average distance between dyad members with that interaction level) to obtain a dimensionless measure $\bar{r}_b$ that better captures the relative distance between the single and the dyad members. In particular, an $\bar{r}_b$ value smaller than 0.5 indicates that the single would have passed through the dyad.

4. Results

4.1. Undisturbed situations

While pedestrians typically aim to minimise travel distance by choosing the straightest path possible, expecting them to walk in a perfectly straight line is unrealistic, even in the absence of other pedestrians. Therefore, we begin by examining the deviation of singles and dyads in 4 m long undisturbed segments, arguing that these segments provide a baseline for expected deviation in the absence of encounters.

In Figs. 6a to 8a, we display the deviation amounts in terms of various deviation measures (see Section 3.5). Additionally, we present in Figs. 6b to 8b the normalised values, obtained by dividing the average deviation of each dyad category (or singles) by the

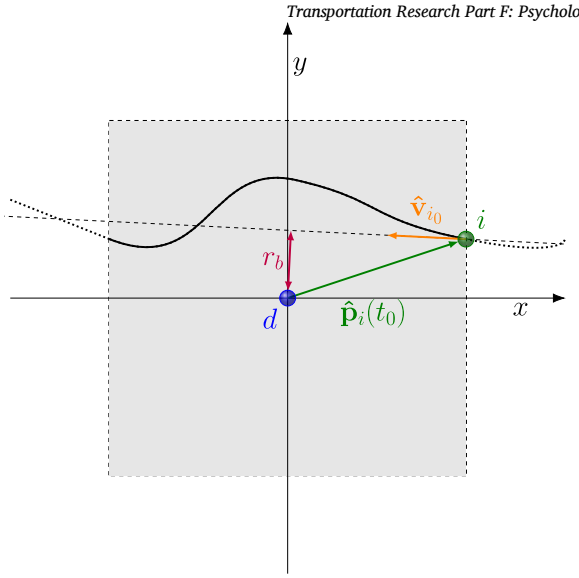

Fig. 5. Impact parameter. Single i in green approaches the dyad d in blue (static and centred at the origin) in a reference frame that moves with the dyad. The gray area represents the 4 m window around the dyad. The (transformed) trajectory of the single inside the box is represented in thick black. The impact parameter r_b indicates the distance between the dyad and the line guided by the single's velocity vectors at the beginning of the encounter.

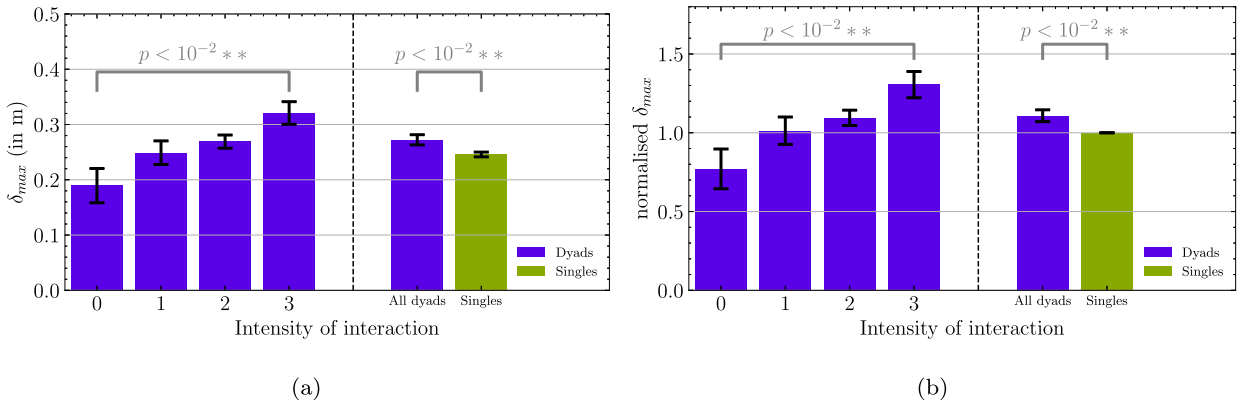

Fig. 6. Lockstep maximum deviation δ_{max} in undisturbed situations. (a) Raw values of δ_{max} for dyads and singles in undisturbed situations. (b) Ratios of the measure to the deviation value for singles. The error bars represent the standard error of the mean. The Kruskal–Wallis p-value for the difference in means between the levels of interaction for the dyads and the Welch T-test p-value for the difference in means between the dyads and the singles are also shown.

average deviation of singles. This normalisation facilitates a straightforward comparison between dyads and singles. Furthermore, we include the Kruskal–Wallis H test p-value for assessing the difference in means among dyads with varying interaction levels, as well as the Welch T-test p-value for comparing the means between singles and all dyads (Kruskal & Wallis, 1952; Welch, 1947). The significance level is set to 0.05 for all tests, and p-values below this threshold are reported in bold in the tables. In the figures, the significance level is indicated by the following symbols: $*$ for $p < 0.05$, $**$ for $p < 0.01$, $***$ for $p < 0.001$ and $****$ for $p < 0.0001$.

The initial noteworthy observation from Figs. 6 to 8 is that deviation is systematically higher for dyads compared to singles, and significantly so for the lockstep maximum deviation δ_{max} (with $H(3) = 16.24$, $p < 10^{-2}$). However, to accurately interpret this observation, it is essential to compare deviations among dyads with varying interaction levels. Examining the breakdown of normalised deviations according to the interaction level of the dyad, we observe a trend where the interaction level correlates with an increase in deviation. Interestingly, non-interacting dyads tend to have smaller deviations than singles, while interacting dyads exhibit comparable or higher deviations.

4.2. Deviations during encounters

We now focus on encounter situations, where dyads and singles pass each other frontally at a distance less than 4 m (Gérin-Lajoie et al., 2005; Cinelli & Patla, 2008; Kitazawa & Fujiyama, 2009). Figs. 9a to 11a present the deviation amounts for both singles and dyads. It is crucial to emphasise that, when reporting deviations in these encounter scenarios, we categorise not only the values of dyads but also those of singles, with respect to the level of social interaction of the dyad involved in that encounter.

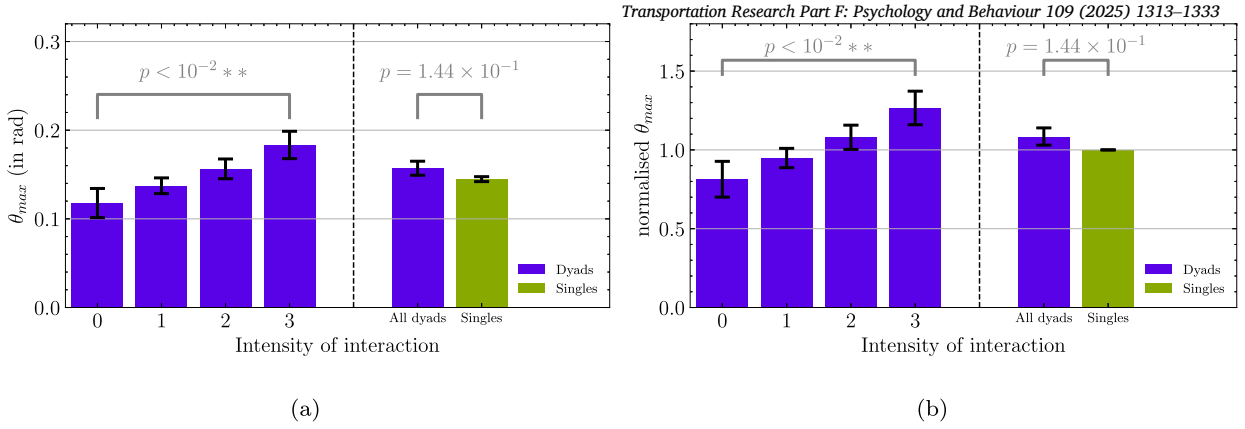

Fig. 7. Maximum cumulative turning angle θ_{max} in undisturbed situations. (a) Raw values of θ_{max} for dyads and singles in undisturbed situations. (b) Ratios of the measure to the deviation value for singles. The error bars represent the standard error of the mean. The Kruskal–Wallis p-value for the difference in means between the levels of interaction for the dyads and the Welch T-test p-value for the difference in means between the dyads and the singles are also shown.

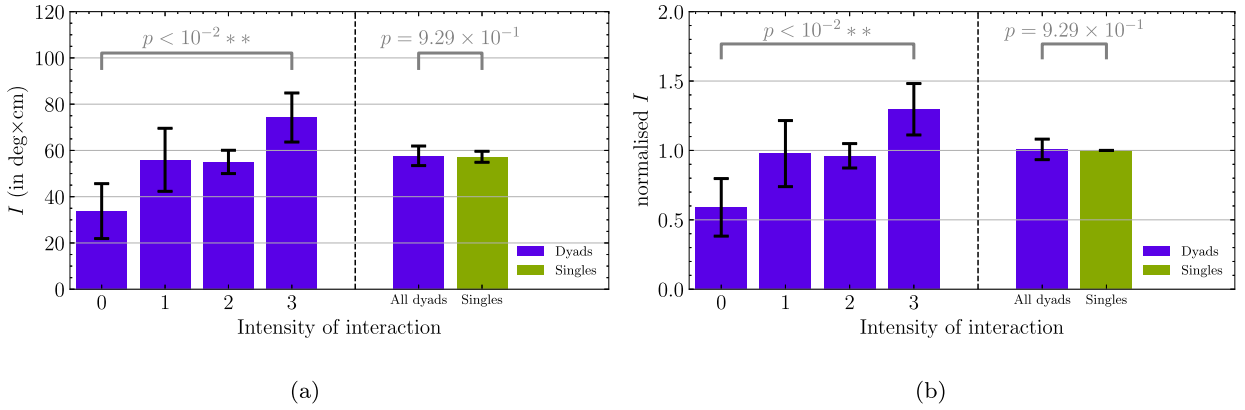

Fig. 8. Turn intensity I in undisturbed situations. (a) Raw values of I for dyads and singles in undisturbed situations. (b) Ratios of the measure to the deviation value for singles. The error bars represent the standard error of the mean. The Kruskal–Wallis p-value for the difference in means between the levels of interaction for the dyads and the Welch T-test p-value for the difference in means between the dyads and the singles are also shown.

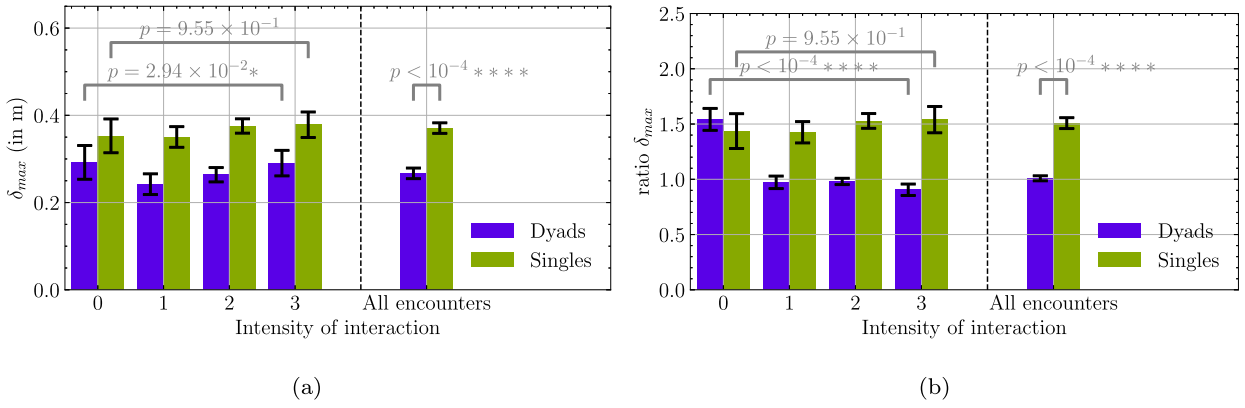

Fig. 9. Lockstep maximum deviation δ_{max} during encounters. (a) Raw values of δ_{max} for dyads and singles in encounters. (b) Ratios of the measure during encounters to the undisturbed value. The error bars represent the standard error of the mean. The Kruskal–Wallis p-value for the difference in means between the levels of interaction for the dyads and the Welch T-test p-value for the difference in means between the dyads and the singles are also shown.

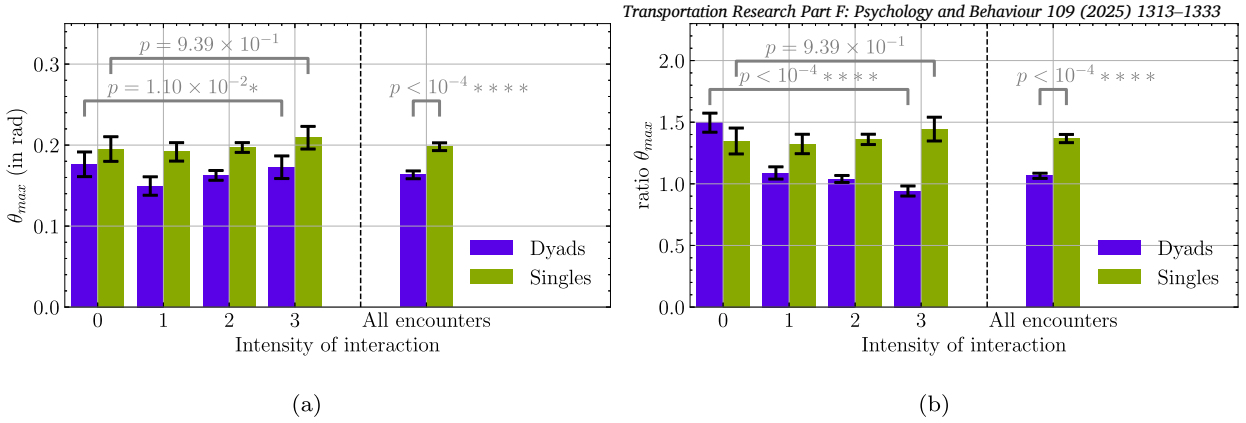

Fig. 10. Maximum cumulative turning angle θ_{max} during encounters. (a) Raw values of θ_{max} for dyads and singles in encounters. (b) Ratios of the measure during encounters to the undisturbed value. The error bars represent the standard error of the mean. The Kruskal–Wallis p-value for the difference in means between the levels of interaction for the dyads and the Welch T-test p-value for the difference in means between the dyads and the singles are also shown.

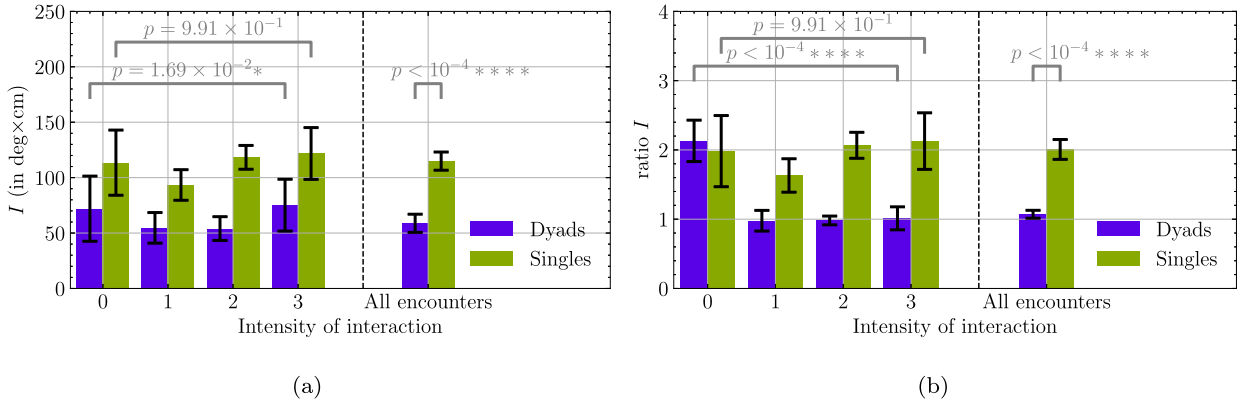

Fig. 11. Turn intensity I during encounters. (a) Raw values of I for dyads and singles in encounters. (b) Ratios of the measure during encounters to the undisturbed value. The error bars represent the standard error of the mean. The Kruskal–Wallis p-value for the difference in means between the levels of interaction for the dyads and the Welch T-test p-value for the difference in means between the dyads and the singles are also shown.

We notice that singles tend to deviate more when encountering dyads with medium or high interaction levels (i.e. levels 2, 3) compared to when they encounter non- or weakly interacting dyads (i.e. levels 0, 1). However, this tendency lacks statistical significance ($H(3) = 0.33$, $p = 0.96$ for δ_{max}, $H(3) = 0.94$, $p = 0.41$ for θ_{max} and $H(3) = 0.99$, $p = 0.11$ for I). Conversely, the variation in dyad deviation is statistically significant ($H(3) = 8.99$, $p = 2.94 \times 10^{-2}$ for δ_{max}, $H(3) = 11.14$, $p = 1.10 \times 10^{-2}$ for θ_{max} and $H(3) = 10.20$, $p = 1.69 \times 10^{-2}$ for I), but no clear pattern emerges, as dyads at interaction levels 0 and 3 deviate more than at levels 1 and 2. Finally, at all interaction levels, the deviations are notably asymmetric, with singles deviating more than dyads in a statistically significant manner.

4.3. Comparison of deviations during encounters and undisturbed situations

The conclusions drawn from the raw values become clearer when juxtaposed with undisturbed situations. To facilitate this comparison, Figs. 9b to 11b provide the ratio of average deviations during encounters to those observed in undisturbed scenarios.

For singles, deviation increases when encountering dyads compared to undisturbed scenarios, with ratios consistently greater than 1. A similar increase is noted for dyads with 0 interaction level, whereas higher interaction levels show ratios close to 1, suggesting minimal change. For dyads, we observe a decrease in the ratios with increasing interaction levels, with statistically significant differences between these interaction levels (Kruskal–Wallis p-values of $H(3) = 42.92$, $p < 10^{-4}$ for δ_{max}, $H(3) = 49.83$, $p < 10^{-4}$ for θ_{max} and $H(3) = 32.84$, $p < 10^{-4}$ for I). Additionally, a statistically significant difference was evident between the deviation ratios of singles and dyads after averaging across all interaction levels for all measures (Welch T-test p-values of $t(875.45) = 9.18$, $p < 10^{-4}$ for δ_{max}, $t(1111.56) = 7.67$, $p < 10^{-4}$ for θ_{max} and $t(806.62) = 6.06$, $p < 10^{-4}$ for I).

These findings are further clarified by Tables 2 to 4, which provide Welch T-test p-values for the difference between undisturbed situations and encounters for both singles and dyads across all interaction levels. Upon averaging over different interaction levels, both singles and dyads exhibited a statistically significant difference between undisturbed and encounter scenarios. However, while

Table 2
Comparison of lockstep maximum deviation between undisturbed situations and encounters. Welch T-test p-values for the difference in means of the lockstep maximum deviation δ_{max} between singles (resp. dyads) in undisturbed situations and singles (resp. dyads) during encounters. Values in bold indicate statistical significance ($p < 0.05$).

Intensity of interaction	Singles	Dyads
0	$\mathbf{9.23 \times 10^{-3}}$	$\mathbf{9.54 \times 10^{-3}}$
1	$\mathbf{< 10^{-4}}$	7.91×10^{-1}
2	$\mathbf{< 10^{-4}}$	7.14×10^{-1}
3	$\mathbf{< 10^{-4}}$	2.52×10^{-1}
All	$\mathbf{< 10^{-4}}$	$\mathbf{6.69 \times 10^{-4}}$

Table 3
Comparison of maximum cumulative turning angle between undisturbed situations and encounters. Welch T-test p-values for the difference in means of the lockstep maximum deviation θ_{max} between singles (resp. dyads) in undisturbed situations and singles (resp. dyads) during encounters. Values in bold indicate statistical significance ($p < 0.05$).

Intensity of interaction	Singles	Dyads
0	$\mathbf{2.35 \times 10^{-3}}$	$\mathbf{5.12 \times 10^{-3}}$
1	$\mathbf{1.38 \times 10^{-4}}$	2.84×10^{-1}
2	$\mathbf{< 10^{-4}}$	6.07×10^{-1}
3	$\mathbf{< 10^{-4}}$	5.36×10^{-1}
All	$\mathbf{< 10^{-4}}$	$\mathbf{3.27 \times 10^{-4}}$

Table 4
Comparison of turn intensity between undisturbed situations and encounters. Welch T-test p-values for the difference in means of the turn intensity I between undisturbed singles (resp. dyads) and singles (resp. dyads) during encounters. Values in bold indicate statistical significance ($p < 0.05$).

Intensity of interaction	Singles	Dyads
0	6.59×10^{-2}	$\mathbf{2.04 \times 10^{-2}}$
1	$\mathbf{1.20 \times 10^{-2}}$	9.38×10^{-1}
2	$\mathbf{< 10^{-4}}$	8.70×10^{-1}
3	$\mathbf{7.48 \times 10^{-3}}$	9.55×10^{-1}
All	$\mathbf{< 10^{-4}}$	$\mathbf{< 10^{-4}}$

the discrepancy remained true for singles regardless of the interaction level of the encountered dyad, only dyads with an interaction level of 0 exhibit a distinct behaviour in encounters compared to undisturbed situations across all three deviation measures.

4.4. Examination in light of the impact parameter

As discussed in Section 3.6, the impact parameter r_b is used to assess how close a single would pass a dyad without any collision avoidance behaviour involved. In particular, $\bar{r}_b$ serves as a dimensionless measure for the initial risk of collision, representing the distance between the single and the dyad relative to the dyad's width (i.e. the average distance between dyad members with that interaction level). We classified $\bar{r}_b$ into four equally sized bins: a value of $\bar{r}_b$ smaller than 1 indicates that the single is on track to pass through or collide with the dyad. Values between 1 and 2 indicate proximity to the dyad but no imminent collision. Between 2 and 3, the single is further away from the dyad, likely requiring minimal deviation to pass comfortably. Finally, a value of $\bar{r}_b$ greater than 3 indicates that the single is far from the dyad and does not need to deviate.

In Figs. 12 to 14, we illustrate the ratio of the average deviation during encounters to the average deviation in undisturbed situations for singles and dyads with respect to the normalised impact parameter $\bar{r}_b$ for each measure. We also provide the Welch T-test p-values for the difference in the ratio between dyads with low interaction levels (0 and 1) versus those with high interaction levels (2 and 3) for each bin of $\bar{r}_b$.

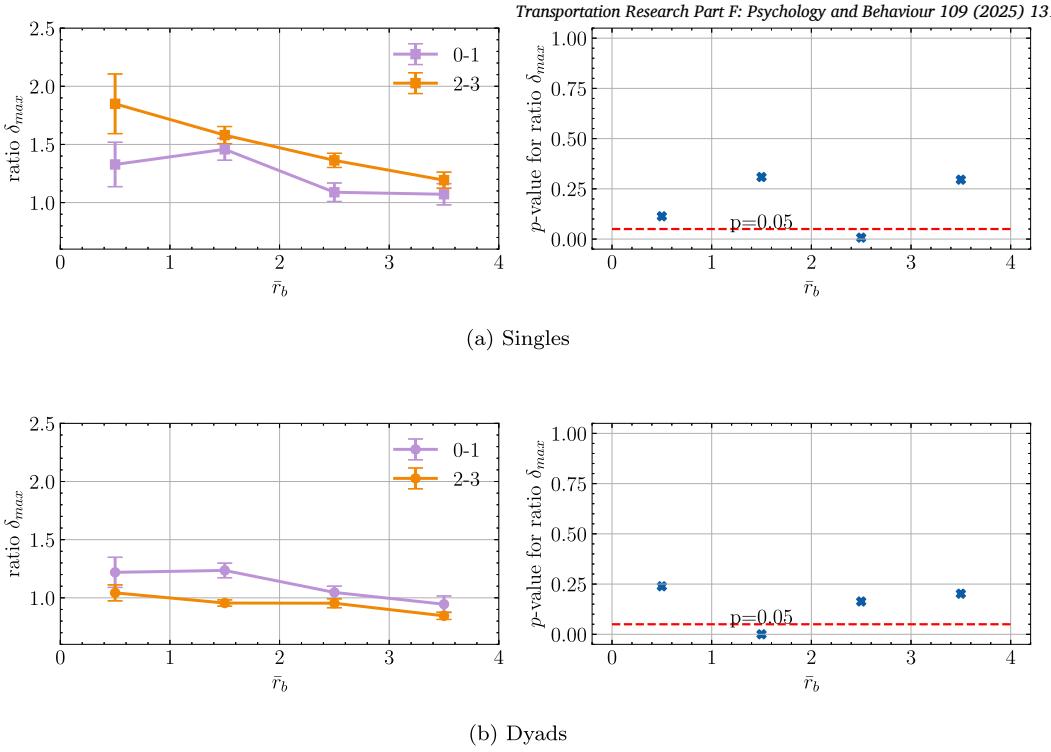

(a) Singles

(b) Dyads

Fig. 12. Lockstep maximum deviation and impact parameter. Ratio of the value of the lockstep maximum deviation of (a) singles and (b) dyads in encounters to the undisturbed value for the binned normalised impact parameter $\bar{r}_b$. The ratios are shown separately for encounters involving dyads with a low (0–1, in blue) and high (2–3, in green) interaction level. The error bars represent the standard error of the mean. The p-values for the difference in means between 0–1 and 2–3 are also shown. The red dashed line represents the significant threshold of $p = 0.05$.

We classified encounters into two groups based on dyads' interaction levels: one with levels 0 and 1, and another for levels 2 and 3. This approach balances the number of data points, ensuring comparable sample sizes. We deem that this categorisation is reasonable as it allows us to contrast low and high interaction levels.

For all deviation measure, both for singles and for dyads, we notice that in the fourth bins of $\bar{r}_b$, the ratios are very close to 1, regardless of the interaction level, indicating no effect of the encounter. At lower values of $\bar{r}_b$, singles and, to a lesser extent, dyads with 0–1 interaction levels show ratios greater than 1. Conversely, ratios for dyads with 2–3 interaction levels remain close to 1, confirming that they are largely unaffected by encounters regardless of collision risk.

Delving deeper into the interaction level effect, we observe that for singles the ratios are higher when encountering dyads with interaction levels 2–3 compared with 0–1 levels. This difference is particularly pronounced in the first bin, likely reflecting the "intrusion" phenomenon reported previously in Gregorj et al. (2023), where singles may choose to pass through non- or weakly interacting dyads instead of deviating. By contrast, the difference in the third bin could be attributed to the fact that for such a value of $\bar{r}_b$ there is no need of avoidance if, as with 0–1 interaction levels, the dyad moves straight (resulting in a ratio around 1). However, when encountering dyads with interaction levels 2–3, singles may need to deviate more, even for such values of $\bar{r}_b$, due to the more unpredictable, "wandering" behaviour of the interacting dyads.

For the dyads, in accordance with the previous results, we observe that the ratio of the lower interaction levels (0–1) is systematically higher for higher interaction levels (2–3) across all measures and all values of $\bar{r}_b$. Finally, the difference in the ratio between the two dyad categories is statistically significant in the second bin of $\bar{r}_b$ (i.e. where the single is close to the dyad but not on a collision course) for all three measures. The more pronounced difference observed in the second bin, compared to the first, may again be attributed to the intrusion phenomenon, which could attenuate the amount of avoidance performed by dyads in the first bin of $\bar{r}_b$, but not in the second.

5. Discussion

In undisturbed situations, non- and weakly interacting deviate significantly less than singles (see Figs. 6 to 8). This indicates that dyads maintain a straighter trajectory compared to singles, potentially owing to their tendency to remain physically close, thereby constraining deviations from the intended path. Using a physical analogy, the inertia of systems composed of the two members is likely greater than that of singles, which would make the dyads more stable.

In addition, awareness of the environmental changes is thought to be linked to dyad's interaction level. It seems reasonable to assume that non- or weakly interacting dyads in undisturbed situations are more attentive to their surroundings, since they do not

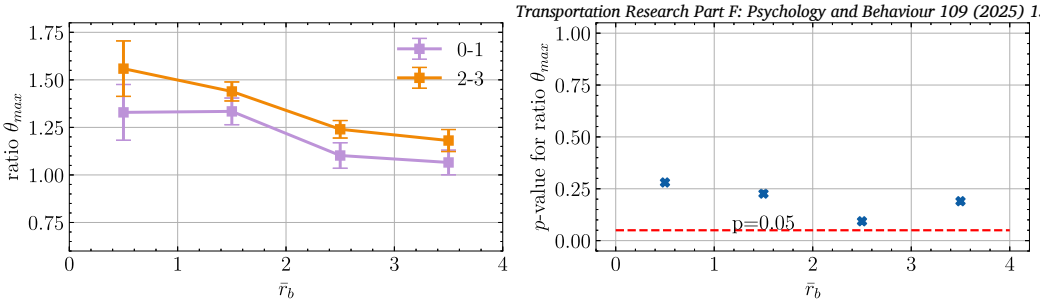

(a) Singles

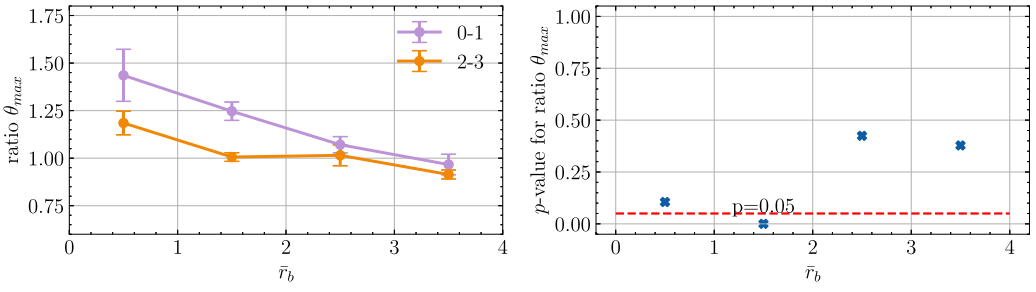

(b) Dyads

Fig. 13. Maximum cumulative turning angle and impact parameter. Ratio of the value of the maximum cumulative turning angle of (a) singles and (b) dyads in encounters to the undisturbed value for the binned normalised impact parameter $\bar{r}_b$. The ratios are shown separately for encounters involving dyads with a low (0–1, in blue) and high (2–3, in green) interaction level. The error bars represent the standard error of the mean. The p-values for the difference in means between 0–1 and 2–3 are also shown. The red dashed line represents the significant threshold of $p = 0.05$.

need to allocate much attention towards social interactions. Consequently, in undisturbed scenarios, these dyads were more likely to choose efficient, straight paths compared to interacting dyads (see Figs. 6 to 8), which may deviate owing to social engagement (interactions).

During encounters, the fact that all dyads deviate significantly less than the singles suggests an asymmetry in avoidance behaviour, with dyads contributing less (see Figs. 9 to 11). In addition, the deviation ratio of non-interacting dyads was significantly higher than that of interacting dyads, suggesting that interaction levels affect dyads' environmental awareness. This is further supported by the fact that the deviation of the singles increases with the dyad's interaction level (see Figs. 9 to 11), although this increase is not statistically significant. This suggests that singles anticipate the reduced involvement of dyads in human–human collision avoidance and adjust their deviations accordingly.

Furthermore, the impact parameter analysis provides further insights into the dynamics of the encounters. The patterns observed in the ratios of deviation during encounters compared to undisturbed situations for singles and dyads with respect to the impact parameter (see Figs. 12 to 14) suggest that the initial collision risk influences the deviation of both singles and dyads. A low impact parameter implies a collision course between the dyad and the single, while higher values suggest safer passing paths. Singles displayed straighter trajectories when on a collision course with non- or weakly interacting dyads, likely owing to a higher rate of intrusion, as observed previously (Gregorj et al., 2023). For dyads, the difference between high and low interaction levels is most pronounced when the single and dyad are set to pass close to each other (second bin), with low interaction level dyads showing significantly higher deviations than their high interaction level counterparts. We hypothesise that this reflects the heightened environmental awareness of low interaction level dyads, making them more responsive to the presence of individuals.

6. Conclusion

Over the last few decades, numerous human–human collision avoidance models have emerged, offering insights into various aspects of pedestrian behaviour (Seyfried et al., 2006; Karamouzas et al., 2014). Despite this extensive body of work, most microscopic models predominantly focus on one-on-one collision avoidance scenarios, often neglecting the dynamics involving groups (Nicolas & Hassan, 2023). This oversight is notable considering that groups comprise a substantial portion of crowds in real-world settings (Schultz et al., 2014; Moussaïd et al., 2010). Therefore, investigating how groups and singles interact during collision avoidance is important for a more comprehensive understanding of pedestrian behaviour. Our study starts to address this gap by investigating how dyads and singles navigate and avoid collisions in crowded environments. In particular, by analysing ecological data and considering various deviation measures, this study presents findings on the stability and deviation dynamics of dyads and singles. Since these

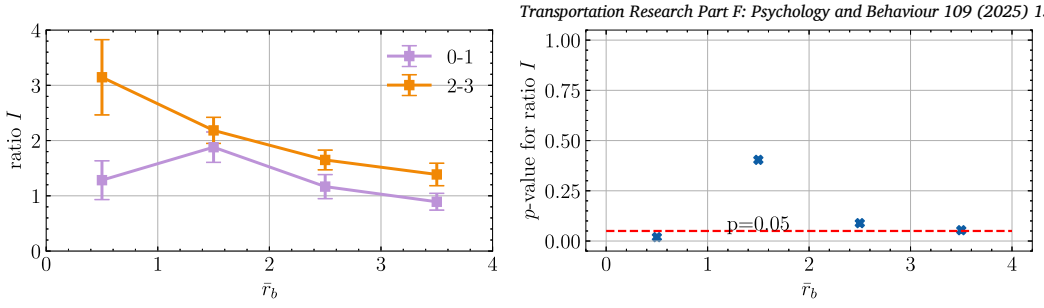

(a) Singles

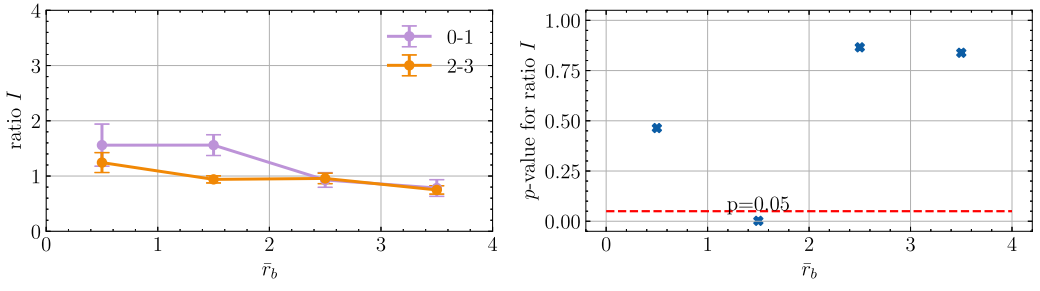

(b) Dyads

Fig. 14. Turn intensity and impact parameter. Ratio of the value of the turn intensity of (a) singles and (b) dyads in encounters to the undisturbed value for the binned normalised impact parameter $\bar{r}_b$. The ratios are shown separately for encounters involving dyads with a low (0–1, in blue) and high (2–3, in green) interaction level. The error bars represent the standard error of the mean. The p-values for the difference in means between 0–1 and 2–3 are also shown. The red dashed line represents the significant threshold of $p = 0.05$.

components serve as the fundamental building blocks of larger groups, it is crucial to understand their interactions as a foundation for understanding more complex group dynamics.

Our analysis shows that social interaction significantly impacts the path deviations of both singles and dyads. In undisturbed scenarios, interacting dyads exhibit larger deviations compared to non-interacting dyads and singles, likely due to reduced attentiveness to their surroundings. During encounters, single pedestrians are the primary contributors to collision avoidance and they adapt their paths based on the interaction level within the dyad, making larger deviations when engaging with highly interactive dyads. Additionally, dyads engaged in social interaction are less responsive to collision risks, relying more on singles for avoidance, which may result from a focus shift toward their social interaction. Finally, we observed significant behavioural differences in path deviations based on the perceived collision risk. Pedestrians, whether walking alone or in groups, exhibit more pronounced deviations when the collision risk is high. The level of social interaction within a dyad seems to play a role in this behaviour. Highly interacting dyads show less deviation when on a path that brings them close to singles, although not directly on a collision course. In contrast, the single tend to deviate more, likely to avoid disrupting their interaction and compensate for the dyad's reduced awareness. This risk-based adjustment is considered an adaptive behaviour, enabling pedestrians to navigate safely in crowded or unpredictable environments.

Nonetheless, our results are not definitive enough to presume a "Theory of Mind" effect (i.e. singles' awareness of the dyad's inner state). Singles may simply be dynamically reacting to the dyad's limited response.

This study offers valuable insights into group-single collision avoidance, highlighting the importance of social interaction in pedestrian dynamics. These findings have practical implications for urban planning, crowd management, and smart systems. They can inform the development of more efficient pedestrian flow strategies and enhance urban space design for greater safety and functionality. Furthermore, the results can support the development of intelligent systems for autonomous vehicles and robots, enabling safer, more seamless interactions with pedestrians in smart environments.

While previous research has suggested that utilising angular variables (Murakami et al., 2021; Fajen, 2013) or velocity adjustments (Huber et al., 2014; Yamamoto et al., 2019) to assess deviations from the intended path could be promising, we faced difficulties in this area. As discussed in Section 3.1, the trajectory data we utilised may not be suitable for computing acceleration, making certain measures (such as the suddenness of turn, the energy curvature or the sinuosity) less effective in capturing deviations compared to others. While controlled experiments can employ various wearable sensors to accurately register position or acceleration (Ikeda et al., 2010; Kaji & Kawaguchi, 2016) implementing such methods in real-world settings poses challenges. Environmental sensors may be sparse or susceptible to measurement noise and clutter, complicating the derivation of accurate values in natural environments.

Another limitation of this study stems from the fact that, although we expect attentional demands to be influenced by the level of interaction between dyad members, we do not directly measure attentional demand or cognitive load. Instead, interaction level

is used as a proxy to infer these effects. This approach, while insightful, necessitates cautious interpretation, as it relies on indirect measures. Future research would benefit from incorporating direct assessments of cognitive load or attentional resources to more precisely understand their influence on dyad behaviour and their role in shaping the observed patterns.

Future research may explore how deviation evolves over time, e.g. incorporating factors like the time or distance to the predicted collision point (Bhojwani et al., 2022; Olivier et al., 2012) or what happens in different situations such as overtaking or following others. It would also be interesting to investigate how the findings of this study might scale to triads or even larger groups. Interaction dynamics in larger groups are more complex, making it challenging to define interaction levels. Force-based models suggest that larger groups exert stronger collective repulsive forces, potentially causing greater deviations in single pedestrians. Additionally, their broader physical span may require singles to deviate more. However, large groups often break into smaller sub-groups (Zanlungo & Kanda, 2013), which may allow singles to pass between them with minimal deviation or disruption. Analysing such scenarios may require defining nested interaction levels to capture the complexity of group dynamics accurately.

Finally, the geometry considered in this study (i.e. a straight corridor) is a simple case that does not capture all the complexities of real-world environments. Extending the study to more complex geometries, such as spaces in which even undisturbed pedestrians may be expected to walk in curved paths, like those studied in van der Vleuten et al. (2024), would be beneficial. This would require a more sophisticated approach to handle the intended paths of pedestrians, as these are likely to be more complex than the straight lines that we considered in this study.

CRediT authorship contribution statement

Adrien Gregorj: Writing – review & editing, Writing – original draft, Visualization, Software, Methodology, Investigation, Formal analysis, Data curation, Conceptualization. **Zeynep Yücel:** Writing – review & editing, Writing – original draft, Supervision, Methodology, Investigation, Formal analysis, Data curation, Conceptualization. **Francesco Zanlungo:** Writing – review & editing, Writing – original draft, Methodology, Investigation, Formal analysis, Data curation, Conceptualization. **Takayuki Kanda:** Writing – review & editing, Project administration, Funding acquisition.

Funding

This work was financially supported by the JSPS Grant-in-Aid for JSPS Fellows 22J20686 and the JSPS KAKENHI Grant Number 23K11169. This work was in part supported by JST Moonshot R and D under Grant Number JPMJMS2011, Japan, and in part supported by JSPS KAKENHI Grant No. 24H00722, Japan.

Acknowledgement

The authors would like to thank Enago (www.enago.com) for the English language review.

Data availability

Code and data have been shared at the “Attach Files” step

dyad-single-encounters-article (Original data) (Zenodo)

References

Bae, J. W., Kim, J., Yun, J., Kang, C., Choi, J., Kim, C., Lee, J., Choi, J., & Choi, J. W. (2023). SiT dataset: Socially interactive pedestrian trajectory dataset for social navigation robots. In A. Oh, T. Naumann, A. Globerson, K. Saenko, M. Hardt, & S. Levine (Eds.), *Advances in neural information processing systems, Vol. 36* (pp. 24552–24563). Curran Associates, Inc.

Ballerini, M., Cabibbo, N., Candelier, R., Cavagna, A., Cisbani, E., Giardina, I., Lecomte, V., Orlandi, A., Parisi, G., Procaccini, A., et al. (2008). Interaction ruling animal collective behavior depends on topological rather than metric distance: Evidence from a field study. *Proceedings of the National Academy of Sciences of the United States of America*, *105*(4), 1232–1237. https://doi.org/10.1073/pnas.0711437105.

Baqui, M., & Löhner, R. (2019). Pedpiv: Pedestrian velocity extraction from particle image velocimetry. *IEEE Transactions on Intelligent Transportation Systems*, *21*(2), 580–589. https://doi.org/10.1109/TITS.2019.2899072.

Baron-Cohen, S. (1997). *Mindblindness: An essay on autism and theory of mind*. MIT Press.

Baron-Cohen, S., Leslie, A. M., & Frith, U. (1985). Does the autistic child have a “theory of mind”? *Cognition*, *21*(1), 37–46. https://doi.org/10.1016/0010-0277(85)90022-8.

Bhojwani, T. M., Lynch, S. D., Bühler, M. A., & Lamontagne, A. (2022). Impact of dual tasking on gaze behaviour and locomotor strategies adopted while circumventing virtual pedestrians during a collision avoidance task. *Experimental Brain Research*, *240*(10), 2633–2645. https://doi.org/10.1007/s00221-022-06427-2.

Bonabeau, E. (2002). Agent-based modeling: Methods and techniques for simulating human systems. *Proceedings of the National Academy of Sciences of the United States of America*, *99*(suppl_3), 7280–7287. https://doi.org/10.1073/pnas.082080899.

Bonnemain, T., Butano, M., Bonnet, T., Echeverría-Huarte, I., Seguin, A., Nicolas, A., Appert-Rolland, C., & Ullmo, D. (2023). Pedestrians in static crowds are not grains, but game players. *Physical Review E*, *107*, Article 024612. https://doi.org/10.1103/PhysRevE.107.024612.

Braham, W. W., Lee, J. M., Oskierko-Jeznacki, E., Silverman, B., & Khansari, N. (2019). Spatial concentration of urban assets in the Philadelphia region: An emergy synthesis. *Ecological Modelling*, *401*, 52–68. https://doi.org/10.1016/j.ecolmodel.2019.03.016.

Bugental, D. B. (2000). Acquisition of the algorithms of social life: A domain-based approach. *Psychological Bulletin*, *126*(2), 187. https://doi.org/10.1037/0033-2909.126.2.187.

Calhoun, A. J., Pillow, J. W., & Murthy, M. (2019). Unsupervised identification of the internal states that shape natural behavior. *Nature Neuroscience*, *22*(12), 2040–2049. https://doi.org/10.1038/s41593-019-0533-x.

Cinelli, M. E., & Patla, A. E. (2007). Travel path conditions dictate the manner in which individuals avoid collisions. *Gait & Posture*, *26*(2), 186–193. https://doi.org/10.1016/j.gaitpost.2006.08.012.

Cinelli, M. E., & Patla, A. E. (2008). Locomotor avoidance behaviours during a visually guided task involving an approaching object. *Gait & Posture*, *28*(4), 596–601. https://doi.org/10.1016/j.gaitpost.2008.04.006.

Cisek, P., & Pastor-Bernier, A. (2014). On the challenges and mechanisms of embodied decisions. *Philosophical Transactions of the Royal Society. Series B, Biological Sciences*, *369*(1655), Article 20130479. https://doi.org/10.1098/rstb.2013.0479.

Corbetta, A., & Toschi, F. (2023). Physics of human crowds. *Annual Review of Condensed Matter Physics* [ISSN 1947-5462], *14*(1), 311–333. https://doi.org/10.1146/annurev-conmatphys-031620-100450.

Corbetta, A., Meeusen, J. A., Lee, C-m., Benzi, R., & Toschi, F. (2018). Physics-based modeling and data representation of pairwise interactions among pedestrians. *Physical Review E*, *98*(6), Article 062310. https://doi.org/10.1103/PhysRevE.98.062310.

Corbetta, A., Lee, C-m., Benzi, R., Muntean, A., & Toschi, F. (2017). Fluctuations around mean walking behaviors in diluted pedestrian flows. *Physical Review E*, *95*, Article 032316. https://doi.org/10.1103/PhysRevE.95.032316.

Costa, M. (2010). Interpersonal distances in group walking. *Journal of Nonverbal Behavior*, *34*, 15–26. https://doi.org/10.1007/s10919-009-0077-y.

Cristiani, E., Menci, M., Malagnino, A., & Amaro, G. G. (2023). An all-densities pedestrian simulator based on a dynamic evaluation of the interpersonal distances. *Physica. A* [ISSN 0378-4371], *616*, Article 128625. https://doi.org/10.1016/j.physa.2023.128625.

Cutting, J. E., Vishton, P. M., & Braren, P. A. (1995). How we avoid collisions with stationary and moving objects. *Psychology Review*, *102*(4), 627. https://doi.org/10.1037/0033-295X.102.4.627.

Daamen, W., Hoogendoorn, S., Campanella, M., & Versluis, D. (2014). Interaction behavior between individual pedestrians. In U. Weidmann, U. Kirsch, & M. Schreckenberg (Eds.), *Pedestrian and evacuation dynamics 2012* (pp. 1305–1313). Springer International Publishing.

Dabbs Jr, J. M., & Stokes III, N. A. (1975). Beauty is power: The use of space on the sidewalk. *Sociometry*, 551–557. https://doi.org/10.2307/2786367.

Dam, A., Oberoi, P., Pierson, J., Jeon, M., & Patrick, R. N. C. (2023). Technological and social distractions at unsignalized and signalized campus crosswalks: A multi-stage naturalistic observation study. *Transportation Research. Part F, Traffic Psychology and Behaviour* [ISSN 1369-8478], *97*, 246–267. https://doi.org/10.1016/j.trf.2023.07.003.

Echeverría-Huarte, I., & Nicolas, A. (2023). Body and mind: Decoding the dynamics of pedestrians and the effect of smartphone distraction by coupling mechanical and decisional processes. *Transportation Research. Part C, Emerging Technologies* [ISSN 0968-090X], *157*, Article 104365. https://doi.org/10.1016/j.trc.2023.104365.

Fajen, B. R. (2013). Guiding locomotion in complex, dynamic environments. *Frontiers in Behavioral Neuroscience*, *7*, 85. https://doi.org/10.3389/fnbeh.2013.00085.

Farhan, S., Avalos, M. A., & Rosenblatt, N. J. (2023). Variability of spatiotemporal gait kinematics during treadmill walking: Is there a Hawthorne effect? *Journal of Applied Biomechanics*, *39*(3), 151–156. https://doi.org/10.1123/jab.2022-0185. ISSN: 1065-8483, 1543-2688.

Ferrer, S., Ruiz, T., & Mars, L. (2015). A qualitative study on the role of the built environment for short walking trips. *Transportation Research. Part F, Traffic Psychology and Behaviour* [ISSN 1369-8478], *33*, 141–160. https://doi.org/10.1016/j.trf.2015.07.014.

Fleiss, J. L., Levin, B., & Paik, M. C. (2003). *Statistical methods for rates and proportions*. Wiley, ISBN 9780471445425.

Francis, J., Giles-Corti, B., Wood, L., & Knuiman, M. (2012). Creating sense of community: The role of public space. *Journal of Environmental Psychology*, *32*(4), 401–409. https://doi.org/10.1016/j.jenvp.2012.07.002.

Friesen, K. B., Zhang, Z., Monaghan, P. G., Oliver, G. D., & Roper, J. A. (2020). All eyes on you: How researcher presence changes the way you walk. *Scientific Reports*, *10*(1), 17159. https://doi.org/10.1038/s41598-020-73734-5.

Fruin, J. J. (1971). Designing for pedestrians: A level-of-service concept. *Highway Research Record*, 1–15.

Gérin-Lajoie, M., Richards, C. L., & McFadyen, B. J. (2005). The negotiation of stationary and moving obstructions during walking: Anticipatory locomotor adaptations and preservation of personal space. *Motor Control*, *9*(3), 242–269. https://doi.org/10.1123/mcj.9.3.242.

Gibson, J. J. (2014). *The ecological approach to visual perception*. Psychology Press.

Glas, D. F., Miyashita, T., Ishiguro, H., & Hagita, N. (2009). Laser-based tracking of human position and orientation using parametric shape modeling. *Advanced Robotics*, *23*(4), 405–428. https://doi.org/10.1163/156855309X408754.

Glas, D. F., Ferreri, F., Miyashita, T., Ishiguro, H., & Hagita, N. (2014). Automatic calibration of laser range finder positions for pedestrian tracking based on social group detections. *Advanced Robotics*, *28*(9), 573–588. https://doi.org/10.1080/01691864.2013.879272.

Gregorj, A., Yücel, Z., Zanlungo, F., Feliciani, C., & Kanda, T. (2023). Social aspects of collision avoidance: A detailed analysis of two-person groups and individual pedestrians. *Scientific Reports*, *13*(1), 5756. https://doi.org/10.1038/s41598-023-32883-z.

Gregorj, A., Yücel, Z., Zanlungo, F., & Kanda, T. (2024a). Ecological data reveal imbalances in collision avoidance due to groups' social interaction. Retrieved from arXiv:2406.06084 [physics].

Gregorj, A., Yücel, Z., Zanlungo, F., & Kanda, T. (2024b). Asymmetries in group-individual collision avoidance due to social factors. *Collective Dynamics* [ISSN 2366-8539], *9*, 1–9. https://doi.org/10.17815/CD.2024.150.

Hediyeh, H., Sayed, T., Zaki, M. H., & Mori, G. (2014). Pedestrian gait analysis using automated computer vision techniques. *Transportmetrica A: Transport Science*, *10*(3), 214–232. https://doi.org/10.1080/18128602.2012.727498.

Helbing, D., & Molnár, P. (1995). Social force model for pedestrian dynamics. *Physical Review E*, *51*(5), 4282–4286. https://doi.org/10.1103/PhysRevE.51.4282.

Hessels, R. S., van Doorn, A. J., Benjamins, J. S., Holleman, G. A., & Hooge, I. T. (2020). Task-related gaze control in human crowd navigation. *Attention, Perception, & Psychophysics*, *82*, 2482–2501. https://doi.org/10.3758/s13414-019-01952-9.

Ho, S., Mohtadi, A., Daud, K., Leonards, U., & Handy, T. C. (Feb. 28, 2019). Using smartphone accelerometry to assess the relationship between cognitive load and gait dynamics during outdoor walking. *Scientific Reports*, *9*(1), 3119. https://doi.org/10.1038/s41598-019-39718-w.

Hollingworth, H. L. (1910). The central tendency of judgment. *The Journal of Philosophy, Psychology and Scientific Methods*, *7*(17), 461–469. https://doi.org/10.2307/2012819.

Hoogendoorn, S., & Bovy, P. (2004). Pedestrian route-choice and activity scheduling theory and models. *Transportation Research. Part B: Methodological* [ISSN 0191-2615], *38*(2), 169–190. https://doi.org/10.1016/S0191-2615(03)00007-9.

Huber, M., Su, Y.-H., Krüger, M., Faschian, K., Glasauer, S., & Hermsdörfer, J. (2014). Adjustments of speed and path when avoiding collisions with another pedestrian. *PLoS ONE*, *9*(2), Article e89589. https://doi.org/10.1371/journal.pone.0089589.

Ikeda, T., Ishiguro, H., Glas, D. F., Shiomi, M., Miyashita, T., & Hagita, N. (2010). Person identification by integrating wearable sensors and tracking results from environmental sensors. In *2010 IEEE international conference on robotics and automation* (pp. 2637–2642).

Itti, L., & Koch, C. (2000). A saliency-based search mechanism for overt and covert shifts of visual attention. *Vision Research*, *40*(10–12), 1489–1506. https://doi.org/10.1016/S0042-6989(99)00163-7.

Jia, X., Feliciani, C., Yanagisawa, D., & Nishinari, K. (2019). Experimental study on the evading behavior of individual pedestrians when confronting with an obstacle in a corridor. *Physica. A*, *531*, Article 121735. https://doi.org/10.1016/j.physa.2019.121735.

Kaji, K., & Kawaguchi, N. (2016). Estimating 3D pedestrian trajectories using stability of sensing signal. In *2016 international conference on indoor positioning and indoor navigation (IPIN)* (pp. 1–8).

Kanda, T., & Brščić, D. (2015). Data set: Pedestrian tracking with group annotations. Retrieved from https://dil.atr.jp/ISL/sets/groups/ (visited on 01/30/2024).

Karamouzas, I., Skinner, B., & Guy, S. J. (2014). Universal power law governing pedestrian interactions. *Physical Review Letters*, *113*(23), Article 238701. https://doi.org/10.1103/PhysRevLett.113.238701.

Kendon, A. (1990). *Conducting interaction: Patterns of behavior in focused encounters, Vol. 7*. CUP Archive.
Kirtley, C., Whittle, M. W., & Jefferson, R. J. (1985). Influence of walking speed on gait parameters. *Journal of Biomedical Engineering*, *7*(4), 282–288. https://doi.org/10.1016/0141-5425(85)90055-x.
Kitazawa, K., & Fujiyama, T. (2009). Pedestrian vision and collision avoidance behavior: Investigation of the information process space of pedestrians using an eye tracker. In *Pedestrian and evacuation dynamics 2008* (pp. 95–108). Springer Berlin Heidelberg.
Knorr, A. G., Willacker, L., Hermsdörfer, J., Glasauer, S., & Krüger, M. (2016). Influence of person- and situation-specific characteristics on collision avoidance behavior in human locomotion. *Journal of Experimental Psychology. Human Perception and Performance*, *42*(9), 1332. https://doi.org/10.1037/xhp0000223.
Krippendorff, K. (2004). Reliability in content analysis: Some common misconceptions and recommendations. *Human Communication Research* [ISSN 0360-3989], *30*(3), 411–433. https://doi.org/10.1111/j.1468-2958.2004.tb00738.x.
Kruskal, W. H., & Wallis, W. A. (1952). Use of ranks in one-criterion variance analysis. *Journal of the American Statistical Association*, *47*(260), 583–621. https://doi.org/10.2307/2280779.
Leonard, K. L., & Masatu, M. C. (2010). Using the Hawthorne effect to examine the gap between a doctor's best possible practice and actual performance. *Journal of Development Economics* [ISSN 0304-3878], *93*(2), 226–234. https://doi.org/10.1016/j.jdeveco.2009.11.001.
Löhner, R. (2010). On the modeling of pedestrian motion. *Applied Mathematical Modelling*, *34*(2), 366–382. https://doi.org/10.1016/j.apm.2009.04.017.
McCambridge, J., Witton, J., & Elbourne, D. R. (2014). Systematic review of the Hawthorne effect: New concepts are needed to study research participation effects. *Journal of Clinical Epidemiology* [ISSN 0895-4356], *67*(3), 267–277. https://doi.org/10.1016/j.jclinepi.2013.08.015.
McPhail, C., & Wohlstein, R. T. (1982). Using film to analyze pedestrian behavior. *Sociological Methods & Research*, *10*(3), 347–375. https://doi.org/10.1177/004912418201003007.
Mobbs, D., Wise, T., Suthana, N., Guzmán, N., Kriegeskorte, N., & Leibo, J. Z. (2021). Promises and challenges of human computational ethology. *Neuron*, *109*(14), 2224–2238. https://doi.org/10.1016/j.neuron.2021.05.021.
Moussaïd, M., Perozo, N., Garnier, S., Helbing, D., & Theraulaz, G. (2010). The walking behaviour of pedestrian social groups and its impact on crowd dynamics. *PLoS ONE*, *5*(4), Article e10047. https://doi.org/10.1371/journal.pone.0010047.
Murakami, H., Feliciani, C., Nishiyama, Y., & Nishinari, K. (2021). Mutual anticipation can contribute to self-organization in human crowds. *Science Advances*, *7*(12), Article eabe7758. https://doi.org/10.1126/sciadv.abe7758.
Nicolas, A., & Hassan, F. H. (2023). Social groups in pedestrian crowds: Review of their influence on the dynamics and their modelling. *Transportmetrica A: Transport Science*, *19*(1), Article 1970651. https://doi.org/10.1080/23249935.2021.1970651.
Nummenmaa, L., Hyönä, J., & Hietanen, J. K. (2009). I'll walk this way: Eyes reveal the direction of locomotion and make passersby look and go the other way. *Psychological Science*, *20*(12), 1454–1458. https://doi.org/10.1111/j.1467-9280.2009.02464.x.
Olivier, A.-H., Marin, A., Crétual, A., & Pettré, J. (2012). Minimal predicted distance: A common metric for collision avoidance during pairwise interactions between walkers. *Gait & Posture*, *36*(3), 399–404. https://doi.org/10.1016/j.gaitpost.2012.03.021.
Olivier, A.-H., Marin, A., Crétual, A., Berthoz, A., & Pettré, J. (2013). Collision avoidance between two walkers: Role-dependent strategies. *Gait & Posture*, *38*(4), 751–756. https://doi.org/10.1016/j.gaitpost.2013.03.017.
Papadimitriou, E., Yannis, G., & Golias, J. (2009). A critical assessment of pedestrian behaviour models. *Transportation Research. Part F, Traffic Psychology and Behaviour* [ISSN 1369-8478], *12*(3), 242–255. https://doi.org/10.1016/j.trf.2008.12.004.
Patla, A. E., & Greig, M. (2006). Any way you look at it, successful obstacle negotiation needs visually guided on-line foot placement regulation during the approach phase. *Neuroscience Letters*, *397*(1–2), 110–114. https://doi.org/10.1016/j.neulet.2005.12.016.
Patla, A. E., & Shumway-Cook, A. (1999). Dimensions of mobility: Defining the complexity and difficulty associated with community mobility. *Journal of Aging and Physical Activity*, *7*(1), 7–19. https://doi.org/10.1123/japa.7.1.7.
Patla, A. E., Tomescu, S. S., Greig, M., & Novak, A. (2007). Gaze fixation patterns during goal-directed locomotion while navigating around obstacles and a new route-selection model. In R. P. G. Van Gompel, M. H. Fischer, W. S. Murray, & R. L. Hill (Eds.), *Eye movements* (pp. 677–696). Oxford: Elsevier.
Rio, K. W., Dachner, G. C., & Warren, W. H. (2018). Local interactions underlying collective motion in human crowds. *Proceedings of the Royal Society. Series B, Biological Sciences*, *285*(1878), Article 20180611. https://doi.org/10.1098/rspb.2018.0611.
Ronchi, E. (2021). Developing and validating evacuation models for fire safety engineering. *Fire Safety Journal*, *120*, Article 103020. https://doi.org/10.1016/j.firesaf.2020.103020.
Rosenberg, M., Zhang, T., Perona, P., & Meister, M. (2021). Mice in a labyrinth show rapid learning, sudden insight, and efficient exploration. *eLife*, *10*, Article e66175. https://doi.org/10.7554/eLife.66175.
Saeedpour-Parizi, M. R., Hassan, S. E., Azad, A., Baute, K. J., Baniasadi, T., & Shea, J. B. (2021). Target position and avoidance margin effects on path planning in obstacle avoidance. *Scientific Reports* [ISSN 2045-2322], *11*(1), Article 15285. https://doi.org/10.1038/s41598-021-94638-y.
Savitzky, A., & Golay, M. J. E. (1964). Smoothing and differentiation of data by simplified least squares procedures. *Analytical Chemistry*, *36*(8), 1627–1639. https://doi.org/10.1021/ac60214a047.
Schultz, M., Rößger, L., Fricke, H., & Schlag, B. (2014). Group dynamic behavior and psychometric profiles as substantial driver for pedestrian dynamics. In U. Weidmann, U. Kirsch, & M. Schreckenberg (Eds.), *Pedestrian and evacuation dynamics 2012* (pp. 1097–1111). Springer International Publishing.
Schwartz, D., Fischhoff, B., Krishnamurti, T., & Sowell, F. (2013). The Hawthorne effect and energy awareness. *Proceedings of the National Academy of Sciences of the United States of America*, *110*(38), 15242–15246. https://doi.org/10.1073/pnas.1301687110.
Sedgwick, P., & Greenwood, N. (2015). Understanding the Hawthorne effect. *BMJ*, *351*. https://doi.org/10.1136/bmj.h4672.
Seyfried, A., Steffen, B., & Lippert, T. (2006). Basics of modelling the pedestrian flow. *Physica. A*, *368*(1), 232–238. https://doi.org/10.1016/j.physa.2005.11.052.
Shumway-Cook, A., Patla, A. E., Stewart, A., Ferrucci, L., Ciol, M. A., & Guralnik, J. M. (2002). Environmental demands associated with community mobility in older adults with and without mobility disabilities. *Physical Therapy*, *82*(7), 670–681. https://doi.org/10.1093/ptj/82.7.670.
Stringer, C., Pachitariu, M., Steinmetz, N., Reddy, C. B., Carandini, M., & Harris, K. D. (2019). Spontaneous behaviors drive multidimensional, brainwide activity. *Science*, *364*(6437), Article eaav7893. https://doi.org/10.1126/science.aav7893.
Tao, Y., Both, A., Silveira, R. I., Buchin, K., Sijben, S., Purves, R. S., Laube, P., Peng, D., Toohey, K., & Duckham, M. (2021). A comparative analysis of trajectory similarity measures. *GIScience and Remote Sensing* [ISSN 1548-1603], *58*(5), 643–669. https://doi.org/10.1080/15481603.2021.1908927.
Torralba, A., Oliva, A., Castelhano, M. S., & Henderson, J. M. (2006). Contextual guidance of eye movements and attention in real-world scenes: The role of global features in object search. *Psychology Review*, *113*(4), 766. https://doi.org/10.1037/0033-295X.113.4.766.
Uetake, T. (1992). Can we really walk straight? *American Journal of Physical Anthropology*, *89*(1), 19–27. https://doi.org/10.1002/ajpa.1330890104.
van Basten, B. J., Jansen, S. E., & Karamouzas, I. (2009). Exploiting motion capture to enhance avoidance behaviour in games. In *Motion in games: Second international workshop* (pp. 29–40). Springer.
van der Vleuten, G. G. M., Toschi, F., Schilders, W., & Corbetta, A. (2024). Stochastic fluctuations of diluted pedestrian dynamics along curved paths. *Physical Review E*, *109*, Article 014605. https://doi.org/10.1103/PhysRevE.109.014605.
von Sivers, I., Templeton, A., Künzner, F., Köster, G., Drury, J., Philippides, A., Neckel, T., & Bungartz, H. J. (2016). Modelling social identification and helping in evacuation simulation. *Safety Science* [ISSN 0925-7535], *89*, 288–300. https://doi.org/10.1016/j.ssci.2016.07.001.
Wang, A., Sato, D., Corzo, Y., Simkin, S., Biswas, A., & Steinfeld, A. (2024). TBD pedestrian data collection: Towards rich, portable, and large-scale natural pedestrian data. Retrieved from arXiv:2309.17187 [cs.CV].
Welch, B. L. (1947). The generalization of student's problem when several different population variances are involved. *Biometrika*, *34*(1–2), 28–35. https://doi.org/10.2307/2332510.

Wilson, A. D., & Golonka, S. (2013). Embodied cognition is not what you think it is. *Frontiers in Psychology*, *4*, 58. https://doi.org/10.3389/fpsyg.2013.00058.

Wu, Y., & Li, H. (2022). Signalling security: An observational and game theory approach to inter-pedestrian psychology. *Transportation Research. Part F, Traffic Psychology and Behaviour* [ISSN 1369-8478], *86*, 238–251. https://doi.org/10.1016/j.trf.2022.02.017.

Yamamoto, H., Yanagisawa, D., Feliciani, C., & Nishinari, K. (2019). Body-rotation behavior of pedestrians for collision avoidance in passing and cross flow. *Transportation Research. Part B: Methodological* [ISSN 0191-2615], *122*, 486–510. https://doi.org/10.1016/j.trb.2019.03.008.

Yücel, Z., Salah, A. A., Meriçli, Ç., Meriçli, T., Valenti, R., & Gevers, T. (2013). Joint attention by gaze interpolation and saliency. *IEEE Transactions on Cybernetics*, *43*(3), 829–842. https://doi.org/10.1109/TSMCB.2012.2216979.

Yücel, Z., Zanlungo, F., Ikeda, T., Miyashita, T., & Hagita, N. (2013). Deciphering the crowd: Modeling and identification of pedestrian group motion. *Sensors*, *13*(1), 875–897. https://doi.org/10.3390/s130100875.

Yücel, Z., Zanlungo, F., & Shiomi, M. (2018). Modeling the impact of interaction on pedestrian group motion. *Advanced Robotics*, *32*(3), 137–147. https://doi.org/10.1080/01691864.2017.1421481.

Zanlungo, F., & Kanda, T. (2013). Do walking pedestrians stabily interact inside a large group? Analysis of group and sub-group spatial structure. *Proceedings of the Annual Meeting of the Cognitive Science Society*, *35*(35).

Zanlungo, F., Ikeda, T., & Kanda, T. (2014). Potential for the dynamics of pedestrians in a socially interacting group. *Physical Review E*, *89*, Article 012811. https://doi.org/10.1103/PhysRevE.89.012811.

Zanlungo, F., Brščić, D., & Kanda, T. (2015). Spatial-size scaling of pedestrian groups under growing density conditions. *Physical Review E*, *91*(6), Article 062810. https://doi.org/10.1103/PhysRevE.91.062810.

Zhou, C., Miao, M.-C., Chen, X.-R., Hu, Y.-F., Chang, Q., Yan, M.-Y., & Kuai, S.-G. (2022). Human-behaviour-based social locomotion model improves the humanization of social robots. *Nature Machine Intelligence*, *4*(11), 1040–1052. https://doi.org/10.1038/s42256-022-00542-z.